uOttawa

L'Université canadienne
Canada's university

FACULTÉ DES ÉTUDES SUPÉRIEURES ET POSTOCTORALES

uOttawa

L'Université canadienne
Canada's university

FACULTY OF GRADUATE AND POSDOCTORAL STUDIES

Alenko Šakanović

AUTEUR DE LA THÈSE / AUTHOR OF THESIS

M.Sc. (Biochemistry)

GRADE / DEGREE

Department of Biochemistry, Microbiology and Immunology

FACULTÉ, ÉCOLE, DÉPARTEMENT / FACULTY, SCHOOL, DEPARTMENT

EphrinB2 Reverse Signalling in Endothelial Cell Migration and Actin Remodeling

TITRE DE LA THÈSE / TITLE OF THESIS

Christina Addison

DIRECTEUR (DIRECTRICE) DE LA THÈSE / THESIS SUPERVISOR

CO-DIRECTEUR (CO-DIRECTRICE) DE LA THÈSE / THESIS CO-SUPERVISOR

EXAMINATEURS (EXAMINATRICES) DE LA THÈSE / THESIS EXAMINERS

Christopher Kennedy

Valerie Wallace

Gary W. Slater

LE DOYEN DE LA FACULTÉ DES ÉTUDES SUPÉRIEURES ET POSTDOCTORALES /
DEAN OF THE FACULTY OF GRADUATE AND POSTDOCORAL STUDIES

EphrinB2 Reverse Signaling in Endothelial Cell Migration And Actin Remodeling

Alenko Šakanović

Thesis submitted to the Department of Biochemistry, Microbiology and Immunology in partial fulfillment of the requirements for the degree of Master's of Science

University of Ottawa
Ottawa, Ontario, Canada
2005

Your file Votre référence
ISBN: 0-494-11402-9
Our file Notre référence
ISBN: 0-494-11402-9

Abstract

Angiogenesis, the formation of new blood vessels from preexisting vasculature, is exaggerated in cancer. A ligand that may be involved in angiogenesis is ephrinB2, which upon binding to its cognate receptor on an adjacent cell, becomes phosphorylated on tyrosine residues and transduces an as yet uncharacterized signal inside the cell. To examine reverse signaling pathways mediated by ephrinB2, ephrinB2 mutants were generated in which five tyrosine residues in the cytoplasmic tail were mutated to phenylalanine by site directed mutagenesis to effectively block the putative signal transduction pathways. Upon overexpression of wildtype and mutant ephrinB2 in endothelial cells, cellular phenotype changed drastically, with impeded proliferation and severe impact on actin remodeling. Observed cytoskeletal changes suggested that the Rho-like GTPases were involved in the actin remodeling mediated by the cytoplasmic tail of ephrinB2. Thus, activation of Rac and Rho upon ephrinB2 stimulation with soluble EphB6, a cognate receptor of ephrinB2, was examined. Adenoviral vectors encoding wildype and mutant ephrinB2 were also generated and used to infect endothelial cells. Wounding assays were used to monitor cell migration of ephrinB2 overexpressing cells to characterize the role of ephrinB2 in this process. Our data suggest that ephrinB2 may play an important role in the migration of endothelial cells during angiogenesis and future work will identify the signaling components of this pathway.

Acknowledgements

Thanks to all the people for their support in making this an extremely rewarding journey.

Greatest thanks go to my supervisor Dr. Christina Addison for giving me a chance to work in a great environment, for her continual guidance and support, and putting up with someone as crazy as I am.

I also wish to thank all the Addison lab members, past and present, including Christie and Jane for their technical support, and allana and Brodie for keeping me (in)sane, the entire staff on the third floor of Ottawa Hospital Regional Cancer Centre, BMI Department at the University of Ottawa, and thesis advisory committee members including Dr. Michael McBurney and Dr. John Copland.

And finally, I wish to thank parents Zuhdija and Ranka and my bro Dinko for their continual support and my girlfriend Marilyne for putting-up with me.

Table of Contents

List of figures

Introduction

Angiogenesis involves the generation and growth of new blood vessels from a pre-existing vascular system. The angiogenic process is defined by activation of quiescent endothelial cells in pre-existing blood vessels, followed by the growth, detachment, and migration of endothelial cells, and leading to the dissolution of the vessel basement membrane. The migration, proliferation and organization of endothelial cells then forms new capillary lumina and loops, and subsequent maturation of microvessels follows deposition of a new basement membrane and recruitment of a smooth muscle pericyte lining (Folkman, 1971). Angiogenesis is an important component of certain normal physiological processes such as embryogenesis, wound healing, and the female reproductive cycle. However, it also contributes to some physiological disorders, in particular to tumour growth (Folkman, 1995).

Angiogenesis has been shown to be a rate-limiting step in tumour development (Hanahan and Folkman, 1996). Furthermore, tumours are limited to a growth of 1-2 mm^3 in the absence of blood supply (Gimbrone *et al.*, 1972) and beyond this minimum size, the growing tumour becomes necrotic and apoptotic as a result of nutrient and oxygen deprivation. As the tumour mass enlarges, hypoxic conditions in the growing tumour prevail, resulting in the release of pro-angiogenic factors, such as vascular endothelial growth factor (VEGF), from tumour cells. These angiogenic factors play a direct role in tumour angiogenesis by promoting endothelial

cell proliferation and vascular permeability (Strawn *et al.*, 1996). The newly formed capillaries, comprised from endothelial cells, form throughout the tumour mass to provide nutrients and growth factors for rapid tumour growth, remove waste generated by tumour metabolism, and transport tumour cells to locations far from the primary site to cause tumour metastasis (Folkman, 1990).

The capillary sprouting indicative of angiogenesis can also be induced *in vitro* by cell-surface associated molecules called ephrins and Eph receptors (Adams *et al.*, 1999). The ephrin-Eph system functions in cell-to-cell rather than long-range communications, because Eph receptors and their cognate ephrin ligands are attached to the plasma membrane. The Eph receptor subfamily is the largest within the family of receptor tyrosine kinases and is subdivided into two structurally different subclasses, termed EphA and EphB. EphA receptors (EphA1-A8) bind glycosylphosphatidylinositol-anchored ephrinA ligands (ephrinA1-A5), whereas EphB receptors (EphB1-B6) bind transmembrane ephrinB ligands (ephrin B1-B3).

EphrinB ligands are inserted into the plasma membrane via a transmembrane region followed by a conserved cytoplasmic domain (Adams *et al.*, 1999). It is because of this feature that this ligand-receptor system has a potential to engage in bi-directional signaling (Palmer *et al.*, 2002). Ephrin ligand binding induces Eph receptor forward signaling which involves tyrosine kinase domain activation and transduction of the signal into the receptor-expressing cell (Himanen and Nikolov, 2003). Following cognate EphB receptor binding, the cytoplasmic tail of the ephrinB ligand undergoes rapid phosphorylation on highly conserved tyrosine residues which can then serve as docking sites for other signaling proteins to mediate reverse

signaling in the ligand expressing cell (Holland *et al.*, 1996). Ephrin molecules appear to acquire high stimulating activation towards their cognate Eph receptors when presented in a clustered state (Davis *et al.*, 1994). The state of aggregation could perhaps determine differential signaling responses (Stein *et al.*, 1998). However, in the reverse signaling (receptor activates ligand) ephrinB ligands co-localize in membrane rafts and are co-clustered by EphB receptors (Palmer *et al.*, 2002).

Three of the five tyrosines conserved in the cytoplasmic tails of the ephrinB ligands have been characterized as the major phosphorylation sites in ephrinB1 following engagement with the Eph receptor ectodomain, both *in vitro* and *in vivo* (Kalo *et al.*, 2001). The cytoplasmic tail of ephrinB1, when activated by one of its cognate receptors, EphB2, becomes phosphorylated by Src family kinases (Palmer *et al.*, 2002). Subsequently, Src-homology-2 (SH2) domain-containing proteins, such as Grb4 (growth-factor-receptor-bound protein 4), bind to the phosphorylated residue tyrosine-298 in the cytoplasmic domain of ephrinB1 (Cowan and Henkemeyer, 2001; Bong *et al.*, 2004). In response to activation of this signaling cascade, cells increase focal adhesion kinase (FAK) catalytic activity, redistribute paxillin, lose focal adhesions, round-up, and disassemble F-actin-containing stress fibers. Grb4 consists of one SH2 domain, and three SH3 domains which form high-affinity protein-protein interactions with molecules that have proline-rich segments (Ren *et al.*, 1993). Grb4 SH3 domains bind a unique set of other proteins, such as Cbl associated protein (CAP) that are implicated in cytoskeletal regulation. CAP has been proposed to regulate actin stress fibers and focal adhesions (Ribon *et al.*, 1998).

Several proteins have been identified that bind via their PDZ domain directly to the C-terminus of ephrinB1. PDZ domains were first identified in the neuron-expressed postsynaptic density protein (PSD95) (Cho *et al.*, 1992), its Drosophila homologue discs large tumour suppressor (DlgA) gene product (Woods and Bryant, 1991), and zonula occludens-1 (ZO1), a tight-junction protein (Itoh *et al.*, 1993). These domains comprise ~90 residues that act as modules and scaffolds for protein–protein interactions (Dev, 2004). Although they may be the sole protein interaction domain within a cytoplasmic protein, they are most often found in combination with other protein interaction domains, such as SH3, participating in complexes that facilitate signaling. PDZ domain containing proteins can bind to the carboxyl-terminus of various proteins, or interact with greater versatility through PDZ-PDZ domain interaction where they bind to internal peptide sequences. Furthermore, PDZ domain-mediated interactions can sometimes be modulated in a dynamic way through target phosphorylation (Nourry *et al.*, 2003). EphrinB1 contains a PDZ binding domain consisting of YYKV motif (Lin *et al.*, 1999).

One protein recently identified to bind to the PDZ domain of ephrinB1 was PDZ-RGS3 (Schmucker and Zipursky, 2001; Lu *et al.*, 2001). It contains an N-terminal PDZ domain and C-terminal regulator of G-protein signaling (RGS) domain, and could therefore be characterized as one of the downstream mediators of ephrin mediated reverse signaling. The PDZ domain is both necessary and sufficient for ephrinB binding. RGS domains act as a GTPase activating protein (GAP) for Gα subunits of trimeric G proteins to promote the hydrolysis of GTP to GDP, thus inactivating signaling. RGSs negatively regulate trimeric G protein-coupled signaling

pathways that mediate a multitude of cellular processes regulated by G-protein coupled receptors (DeVries and Farquhar, 1999). PDZ-RGS3 is a protein that regulates trimeric G proteins during cell migration (Lu *et al.*, 2004). A schematic summary of Eph/ephrin signaling is shown in Figure 1.

Cell surface receptors, such as growth factor receptors and adhesion receptors, regulate cell morphology and cell behavior by modulation of the activity of the Rho family of GTPases (Noren and Pasquele, 2004). These GTPases are molecular switches that cycle between an inactive GDP bound state and an active GTP bound state (L. Van Aelst *et al.*, 1997). They are activated by guanine nucleotide exchange factors (GEFs), which promote the exchange of GDP for GTP, and inactivated by GTPase-activating proteins (GAPs), which promote the hydrolysis of GTP to GDP. Activated Rho family proteins bind to downstream effectors to stimulate signaling pathways that influence a multitude of cellular properties, including actin cytoskeleton organization, cell adhesion and migration, and membrane trafficking (Tapon and Hall, 1997; Ridley, 2001). Given the effects of Eph receptors and ephrin ligands on cell shape, adhesion, and migration, it is not surprising that some recent critical evidence has linked the ephrin/Eph signaling pathway to several members of the Rho family (Noren and Pasquele., 2004). The most well characterized members of this family are RhoA, Rac1, and Cdc42. RhoA regulates stress fiber and focal adhesion formation and cell contractility, whereas Rac1 or Cdc42 activation results in the formation of protrusive structures such as lamellipodia and filopodia, respectively. Recently, it has been demonstrated that EphB receptors associate with Intersectin and Kalirin, two exchange factors that activate Cdc42 and Rac1, respectively (Irie and

Yamaguchi, 2002; Penzes *et al.*, 2003). Furthermore, it has been shown that EphB2 cooperates synergistically with neural Wiscott-Aldrich syndrome protein (N-WASP) to activate Intersectin (Cory *et al.*, 2002). Because N-WASP binds to the actin polymerizing complex Arp 2/3 in the presence of activated Cdc42, this provides a direct link from EphB2 receptor activation to actin filament assembly and branching.

The activity of another Rho family member, Rac1, is required for cell spreading and membrane ruffling in human aortic endothelial cells in response to activation of EphB receptors by treatment with soluble dimeric ephrinB1 (Nagashima *et al.*, 2002). In addition to promoting ruffling and lamellipodia protrusion, recent evidence has revealed another function of Rac1 downstream of EphB receptors. Contact between cells expressing EphB receptors and ephrinB ligands leads to a process that most closely resembles localized phagocytosis or micropinocytosis and depends on actin polymerization and dynamin function downstream of activated Rac1 (Marston *et al.*, 2003; Zimmer *et al.*, 2003). Through this process, activated EphB receptors clustered at sites of cell-cell contact are internalized into vesicles together with their bound full-length ephrinB ligands. In contrast with the evidence that EphB receptors activate Rac1 in endothelial cells, ephrinB1 stimulation of EphB receptors in intestinal epithelial cells has been shown to decrease Rac1 activity (Battle *et al.*, 2002). It remains to be determined if EphB receptors signal differentially in some cell types or stimulate Rac1 inactivation only transiently.

Increasing evidence indicates that Eph receptors signal to the actin cytoskeleton via the Rho family of GTPases, however, little is known about the effects of ephrinB reverse signaling on Rho family proteins. Some recent evidence

suggests that Disheveled mediates RhoA activation downstream of ephrinB1 (Tanaka *et al.*, 2003), and its tyrosine phosphorylation and RhoA activation only occur in response to ephrinB1 stimulation by EphB receptors. Another link between ephrinB ligands and RhoA may be the phosphotyrosine phosphatase PTP-BL, which associates with ephrinB upon activation by EphB receptors and also binds p190RhoGAP (Noren and Pasquele, 2004). p190RhoGAP plays an important role in inactivating RhoA downstream of several cell adhesion receptors such as integrins and cadherins (Arthur *et al.*, 2000; Noren *et al.*, 2003). It is, however, unclear if ephrinB reverse signaling activates Rac and Cdc42.

Elevated Eph/ephrin expression is associated with angiogenesis and tumour vasculature in many types of human cancers, including breast, lung, and prostate cancers, melanoma and leukemia (Surawska *et al.*, 2004). Eph receptors and their ephrin ligands have also been implicated in diverse developmental and neurological functions including hindbrain development and tissue patterning. Furthermore, EphB4 and ephrinB2 regulate propulsive and repulsive functions that mediate spatial organization signaling during angiogenesis and vessel assembly (Fuller *et al.*, 2003). In fact, the ligand ephrinB2 plays a significant role in demarcation of arteriole versus venule vessels during embryonic vasculogenesis, such that ephrinB2 marks arterial but not venous endothelial cells and conversely, EphB4, a receptor for ephrinB2, marks veins but not arteries (Wang *et al.*, 1998). Using an *in vitro* endothelial cell sprouting assay, recent results have provided evidence that ephrinB stimulation and signaling mediate angiogenesis (Adams *et al.*, 2001). Furthermore, the observed blood vessel formation and sprouting requires the phosphorylation of the cytoplasmic

domain of ephrinB ligands by the Src family kinases implicating a role for ephrinB reverse signaling in angiogenesis (Palmer *et al.*, 2002).

In order to characterize the poorly understood mechanism of action of ephrinB2, we decided to examine the role of ephrinB2 reverse signaling in angiogenesis. We investigated cellular behaviour upon "artificial" stimulation of reverse signaling and generated and overexpressed ephrinB2 mutants. As previous literature had suggested that Src may mediate the phosphorylation of ephrinB ligands following receptor binding, all tyrosine sites on the cytoplasmic domain of ephrinB2 were treated as potential phosphorylation sites (Figure 2). To date, it is known that the phosphorylated residue tyrosine-304 in the cytoplasmic tail of ephrinB2 confers high affinity and bifunctional binding to both the SH2 domain of Grb4 and the PDZ domain of the PDZ-RGS3 protein (Su *et al.*, 2004) however, downstream signaling and physiological outcomes are poorly understood. Mutations were carried out individually on all five cytoplasmic tyrosines and upon overexpression of these mutants, phenotypic changes were observed. Specific changes that affected cytoskeletal rearrangement, cellular shape, and migration were noted, and as these processes are the outcomes associated with angiogenesis, it suggests a possible role of ephrinB2 in this process.

Figure 1. Schematic representation of Eph/ephrin signaling. Forward signaling is shown in gray, and reverse signaling pathways are shown in colour.

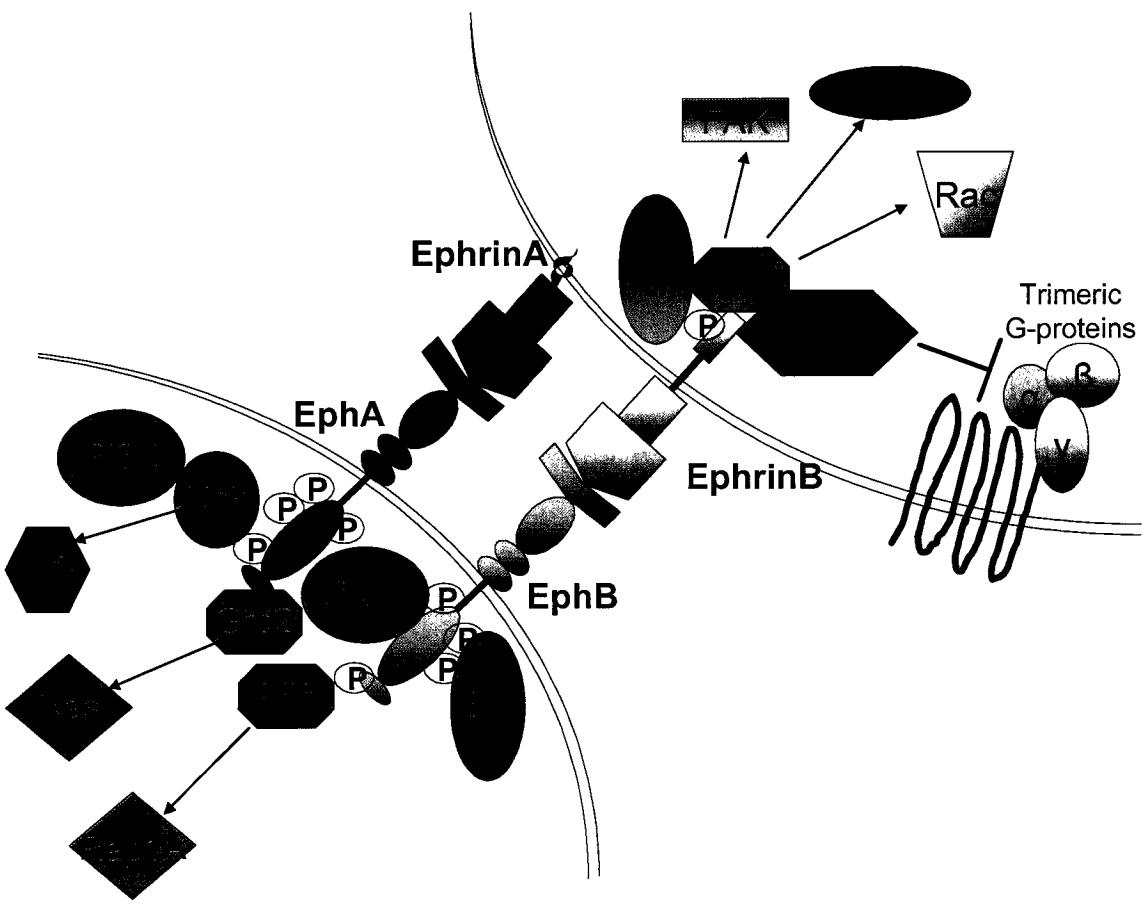
EphrinA
EphA
EphrinB
EphB
Rac
Trimeric
G-proteins
α
β
γ
P

Figure 2. Schematic representation of ephrinB2 protein sequence showing all five cytoplasmic tyrosines as well as the PDZ binding domain.

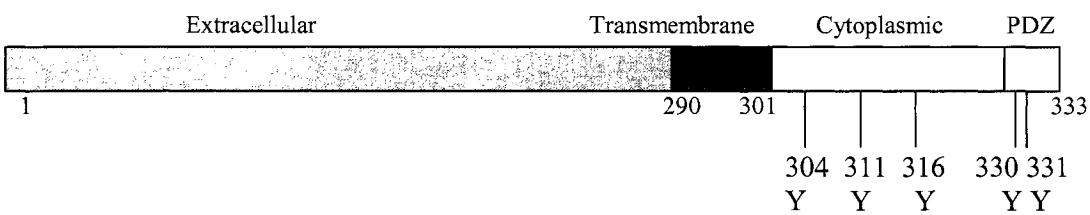
Extracellular
Transmembrane
Cytoplasmic
PDZ
1
290
301
333
304
Y
311
Y
316
Y
330
Y
331
Y

Hypothesis

EphrinB2 expression and activation is required for endothelial migration and organization that occurs during the angiogenic process.

Materials and Methods

Cell Culture. Human dermal microvascular endothelial cells (HDMEC), obtained from Cambrex (East Rutherford, NJ), used from passage 4-8, were grown using EGM-2MV (Cambrex) at 37°C with 5% CO_2. Human umbilical vein endothelial cells (HUVEC), obtained from Cambrex, used from passage 5-14, were grown in EGM-2 (Cambrex) at 37°C with 5% CO_2. Cells were passaged by trypsinization with the exception of when utilized in adhesion assays where cells were removed by incubation with ice-cold 5mM ethylenediaminetetraacetic acid (EDTA) in phosphate buffered saline (PBS) (137mM NaCl, 8.2mM Na_2HPO_4, 1.5mM KH_2PO_4, 2.7mM KCl). Trypsinization of endothelial cells was performed following two washes in Hanks balanced salt solution (HBSS), (Gibco, Grand Island, NY) followed by incubation in a 0.05% solution of trypsin (Sigma, St. Louis, MO) diluted in HBSS at 37°C for approximately 3 minutes or until the cells were lifted off the dish. Cells were then collected and the trypsin was neutralized by addition of an equal amount of media containing fetal bovine serum. A 10µl sample of cells from the suspension was diluted 1:2 in a 4% trypan blue solution and counted on a haemocytometer to calculate the number of cells recovered (cell count/4 x 2 x 10,000 x volume of suspension). Cells were centrifuged (Beckman, Fullerton, CA) at 1100g at 4°C for 5 minutes prior to resuspension in EGM-2MV (HDMEC) or EGM-2 (HUVEC) and seeding in new culture ware (VWR, Mississauga, ON) at a density of 5000 cells/cm^2. Low passage 293 cells (26-35), obtained from Dr. Frank L. Graham were grown in Minimum Essential Media (Gibco) supplemented with 10% fetal

bovine serum (FBS), 100U/ml penicillin/streptomycin, and 2.5μg/ml fungizone and incubated at 37°C with 5% CO_2. When they reached approximately 90% confluency, they were split 1 to 4 (every 3-4 days), by rinsing cell monolayers twice with 3ml of citric saline (135mM KCl, 15mM sodium citrate), followed by incubation at room temperature until cells rounded up and detached from the dish with gentle tapping. Cells were resuspended in complete medium and distributed to new dishes. A confluent 100mm dish was split into eight 60mm dishes for cotransfection which was performed 48 hours later or into two 150mm dishes for high titer viral stock preparation which was performed 72 hours later. Amphotropic PT67 retroviral packaging cells (Clontech, Mountain View, CA) were cultured in Dulbecco's Modified Eagle Medium (DMEM) (Invitrogen, Burlington, ON) supplemented with 10% FBS (Gibco). Cells were grown to confluence, washed twice with phosphate buffered saline (PBS, 137mM NaCl, 8mM Na_2PO_4, 2.7mM KCl), and trypsinized with 0.05% trypsin (Sigma) diluted in PBS. Cells were split 1:4 every 3-4 days and incubated at 37°C with 5% CO_2.

Antibodies and recombinant proteins. Several antibodies were used in this project. Secondary horse radish peroxidase (HRP) -conjugated anti-mouse and anti-goat antibodies were from Sigma (St. Louis, MO). Primary Mouse anti-Rac (clone 23A8) was from Upstate (Lake Placid, NY) and mouse anti-Rho was from Santa Cruz Biotechnologies (Santa Cruz, CA). Anti-mouse ephrinB2 antibody was from R&D Systems (Minneapolis, MN). The anti-tubulin antibody (E7) was produced by a hybridoma cell line that was given to the lab by Dr. D.L. Brown. Recombinant vascular endothelial growth factor 165 ($VEGF_{165}$), epidermal growth factor (EGF)

and basic fibroblast growth factor (bFGF) were purchased from R&D Systems (Minneapolis, MN). Recombinant EphB6-Fc chimera (EphB6 receptor fused to Fc portion of human IgG) was from R&D Systems (Minneapolis, MN), and human IgG was from Sigma (St. Louis, MO).

Recombinant Protein Stimulation. HUVEC were grown to confluence in EGM-2 media on 100mm dishes. They were then washed twice with HBSS, and serum starved overnight in MCDB 131 media. Cells were stimulated with 1, 10, 50 or 250ng/ml of VEGF, EGF or bFGF in MCDB 131 without serum overnight, and subsequently lysed in 300µl of FRAK's buffer (10 mM tris pH 7.5, 150mM NaCl, 5mM EDTA, 1% Triton X-100) supplemented with protease and phosphatase inhibitors (0.2mM sodium orthovanadate, 2mM NaF, 2mM sodium pyrophosphate, 0.2mM phenylmethylsulfonylfluoride, 500uM ammonium vanadate, 2ug/ml aprotinin, 5ug/ml leupeptin). HUVEC were also grown to confluence in EGM-2 media in 60 mm dishes. They were then stimulated with 10, 50 and 250ng/ml of VEGF in MCDB 131 for various times. Two, 8, 24, and 48 hours post stimulation, media was removed and cells were lysed with 500µl of TRIzol reagent (Invitrogen), scraped, put into 15ml conical tubes and frozen at -80°C. RNA was then isolated using phenol/chloroform extraction according to the manufacturer's protocol (Invitrogen).

RT-PCR. Isolated RNA was used as a template for generation of cDNA using the first strand synthesis kit from Fermentas (Burlington, ON) according to the manufacturer's protocol using random hexamer as a primer. cDNA was subsequently used in polymerase chain reaction (PCR) experiments to amplify ephrinB2 (sense

primer: GGACTCTAAAACTGTTGGCCAGT and anti-sense primer: CTTGTTGTCGAACTTCTTCCATTT) and GAPDH (sense primer: CAGTCAAGGCT-GAGAATGGGA and anti-sense primer: TTGATGTCATCATACTTGGCAG) messages using the following conditions: 1X PCR buffer, 0.8mM dNTPs, 1.5mM $MgCl_2$, 5ng/μl each of sense and anti-sense primers, 1U Ampli Taq Gold DNA polymerase (Applied Biosciences, Salt Lake City, UT) at 94°C for 10min, 25X(94°C for 30sec, 56°C for 45sec, 72°C for 1min), 72°C for 7min, 4°C hold for ephrinB2 and 94°C for 10min, 30X(94°C for 30sec, 59°C for 45sec, 72°C for 1min), 72°C for 10min, 4°C hold for GAPDH. To visualize the PCR products, 6X gel loading dye (0.25% bromophenol blue, 0.25% Xylene cyanol FF, 30% glycerol) was added to each sample prior to loading on 1% agarose gels in TAE buffer (40mM Tris-Acetate, 1mM EDTA, pH 8.3) supplemented with 5μg/ml ethidium bromide, and subjecting the samples to electrophoresis at 100V for ~45 minutes or until the PCR products had resolved. Gels were then visualized using Gene Genius gel detection system (SynGene, Cambridge, England).

Plasmids. Dr. Christina Addison previously cloned the cDNA for human ephrinB2 into the pLXSN plasmid to generate pLXSN-EFNB2, which was subsequently used in all of the mutagenesis experiments. Mutated and wild-type ephrinB2 genes were amplified from the pLXSN-EFNB2 plasmid using PCR with the following primers to pLXSN or ephrinB2 sequences: pLXSN reverse primer: TTCCACACCCTAACTGACACAC and forward ephrinB2 primer: AAGCTAGCCCTCACTCCTTCTC. The following cycles were used for amplification by PCR: 94°C for 10min, 5X(94°C for 30sec, 52°C for 45sec, 72°C for

1min), 25X(94°C for 30sec, 59°C for 45sec, 72°C for 1min), 72°C for 10min, 4°C hold. PCR amplification products were separated on 1% agarose gels and a DNA band of ~1.1kb was excised and purified using the Gel Extraction kit (Qiagen, Mississauga, ON) according to manufacturer's protocol. The excised DNA fragment was then inserted into pT7Blue3 Blunt Vector using the Novagen Perfectly Blunt Cloning kit according to the manufacturer's protocol (Novagen, Madison, WI). White bacterial colonies, that are indicative of plasmids containing ligated DNA inserts, were picked and grown in 2ml of Luria-Bertani broth (LB) (1% peptone, 0.5% yeast extract, 160mM NaCl) overnight, and DNA was extracted using the Mini Prep kit (Qiagen) according to manufacturer's protocol. The integrity of the isolated plasmid DNA was verified by XbaI digest and subsequently used to isolate the genes for further cloning. To this end, 5µl of each plasmid containing the appropriate inserts was digested with NheI (5U), and BamHI (5U) overnight at 37°C. In parallel, 1µg of the adenoviral shuttle plasmid pDC315 was also digested with NheI for 5 hours at 37°C, and subsequently BamHI was added for digestion overnight at 37°C. The resulting restriction digests were then separated on a 1% agarose gel and the ~1.1kb fragment of ephrinB2 and ~4kb fragment of pDC315 were gel purified using the Gel Extraction kit as described above. The isolated DNA fragments were then ligated using T4 DNA ligase and incubation overnight at 16°C. Following ligation, DH5α $CaCl_2$ competent bacteria were transformed with the resulting plasmid DNA, allowed to recover following addition of 1ml of LB and incubated at 37°C for 1 hr. Subsequently the transformed bacteria were plated by spreading on LB agar containing 75µg/ml ampicillin and incubated overnight at 37°C to allow bacterial

growth. Isolated bacterial colonies were further grown in LB broth, and the plasmid DNA was isolated using Mini Prep kit (Qiagen) according to manufacturer's protocol. Plasmids containing the appropriate inserts were identified by a predicted DNA fragment pattern following restriction enzyme digestion by EcoRI.

Mutagenesis. All mutagenesis experiments were performed using the PCR based QuickChange XL SiteDirected Mutagenesis Kit according to the manufacturer's recommendations (Stratagene, La Jolla, CA), and specifically designed primers (forward and reverse) for each one of the five mutations. Briefly, 10ng of double stranded plasmid DNA template and 125ng of each primer were used in the reaction. PCR amplification was performed as follows: 95°C for 1min, 18 x (95°C for 50 sec, 55°C for 50 sec, 68°C for 18 min), 68°C for 7 min, 4°C hold. All primers used for mutagenesis were synthesized and PAGE-purified by Sigma (Oakville, ON). Forward and reverse primers for each mutation are shown respectively with the mutation underlined in each case: Y 304 F – C TTC TGC CCT CAC T<u>T</u>C GAG AAG GTC AGC GG, CC GCT GAC CTT CTC G<u>A</u>A GTG AGG GCA GAA G; Y 311 F – G GTC AGC GGG GAC T<u>T</u>C GGG CAC CCG GTG, CAC CGG GTG CCC G<u>A</u>A GTC CCC GCT GAC C; Y 316 F – C GGG CAC CCG GTG T<u>T</u>C ATC GTC CAG GAG, CTC CTG GAC GAT G<u>A</u>A CAC CGG GTG CCC G; Y 330 F – GC CCG GCG AAC ATT T<u>T</u>C TAC AAG GTC TGA G, C TCA GAC CTT GTA G<u>A</u>A AAT GTT CGC CGG GC; Y 331 F – CG GCG AAC ATT TAC T<u>T</u>C AAG GTC TGA GAG GG, CC CTC TCA GAC CTT G<u>A</u>A GTA AAT GTT CGC CG; Y 331 F*- CG GCG AAC ATT TTC T<u>T</u>C AAG GTC TGA GAG GG, CC CTC TCA GAC CTT G<u>A</u>A GAA AAT GTT CGC CG.

Y 331 F* primer was used to generate the mutation on a previously generated Y 330 F plasmid. Mutated plasmids were grown in high transformation efficiency XL-Gold bacterial cells (provided with the kit) according to manufacturer's protocol (Stratagene), Plasmids were purified using Qiagen Mini-Prep kit, and confirmed by sequencing by Cortec (Kingston, ON).

Generation and propagation of Adenoviral vectors. Adenoviral (Ad) vectors were generated using the two-plasmid cotransfection method in 293 cells as previously described (Ng and Graham, 2002). Briefly, 2.5μg of adenoviral vector shuttle plasmid pDC315, into which the ephrinB2 cDNAs had previously been inserted, together with 5μg of pBHGΔE1,3loxP (both from Microbix Biosystems, Toronto, ON) were mixed together in 0.5ml of HeBS buffer (21mM HEPES, 137mM NaCl, 5mM KCl, 0.7mMNa_2HPO_4, 5.5mM glucose, pH 7.1), containing 10μg/ml of sheared salmon sperm DNA (Invitrogen) (generated following vigorous vortexing for 2 minutes) in 15ml conical tubes. As a positive control for the efficiency of cotransfection, 1μg of the infectious Ad genomic plasmid pFG140 was used as a control. To this mixture, 50μl of a 2.5M $CaCl_2$ solution was added drop-wise with gentle shaking and the tubes were incubated for 30 minutes at room temperature. Subsequently, 500μl of the precipitated plasmid preparation was added drop-wise to 80-90% confluent 293 cells in 60mm dishes and incubated overnight at 37°C. The next day, a 1:1 solution of 1% agarose in sterile water and 2X Modifed Eagle Media (Gibco) supplemented with 10% horse serum, 200U/ml penicillin/streptomycin, 5μg/ml fungizone, and 0.2% yeast extract was overlayed on the top of the cell monolayers and was left to solidify. Once the gels had formed, the cells were then

incubated at 37°C until viral plaques appeared (3-4 weeks). Adenovirus was obtained from well-isolated plaques following punching of the agarose plug and washing of the plaque with PBS^{++} (PBS, 0.68mM $MgCl_2$, 0.5mM $CaCl_2$) supplemented with 10% glycerol. The isolated viral material was then stored at -80°C. The identity of the isolated virus was determined following infection of 60mm dishes of 90% confluent 293 cells with 200µl of isolated viral plaque material. For infection, media was removed from the cells and the viral inoculate was added to the surface of the cells which were then incubated for 1 hour at 37°C, with rocking every 15 minutes. Following adsorption of the virus, 5ml of supplemented Minimum Essential Media (with 10% FBS, penicillin/streptomycin, and fungizone) was added and cells were incubated at 37°C until complete cytopathic effects (CPE) were observed (>90% cells rounded up and detached from dish, usually 2-3 days post infection). The media was then gently removed with a pipette, leaving the majority of the cells in the dish. The media was transferred to a suitable vial, supplemented with 10% glycerol and stored at -80°C to use as inoculum for subsequent infections. To the remaining cells in the dish, 0.5ml of a pronase-SDS solution (0.5mg/ml pronase, 0.5% SDS, 10mM Tris-HCl pH 7.4, 10mM EDTA, pH 8.0) was added and incubated overnight at 37°C. Lysates were transferred to a microfuge tube and 1ml of 95% ethanol was added to precipitate the released viral DNA. DNA was pelleted by centrifugation, washed twice with 70% ethanol, dried and resuspended in 50µl of TE buffer (10mM Tris-HCl pH 8.0, 1mM EDTA pH 8.0). The isolated DNA was heated at 65°C for 20 minutes, and subsequently 5µl of viral DNA was digested with HindIII enzyme and analyzed by ethidium bromide staining following agarose gel electrophoresis to verify the

DNA structure of the recombinant virus was as expected. Once the identity of the virus isolate was confirmed the glycerol/media stocks of virus was diluted 1:8 in PBS^{++} and 1ml of this dilution was used to infect a 90% confluent 150mm dish of 293 cells as described. Following viral adsorption, 25ml of maintenance medium was added and cells returned to 37°C, and examined daily for signs of CPE. When CPE was nearly complete (most cells rounded but not yet detached), cells were scraped into the medium and centrifuged at 800g for 15 minutes. The resulting cell pellet was resuspended in 2ml of PBS^{++} supplemented with 10% glycerol, and frozen at -80°C (crude viral stock). Serial dilutions (e.g. 10^{-6}, 10^{-7}, 10^{-8}) of crude viral stock were prepared in PBS^{++} in duplicates and used to infect 60mm dishes of 90% confluent 293 cells. After 1 hour of adsorption, dishes were overlayed with 10ml of 1:1 agarose/2X media, left to solidify and incubated at 37°C as previously described. Approximately 12 days post infection, the number of resulting plaques on each dish was counted and the adenoviral vector concentration was calculated as plaque forming units per ml as follows: pfu/ml = (number of plaques)/(dilution factor)(infection volume). Crude viral stocks with known concentrations were used to infect endothelial cells at different multiplicities of infection (MOI). For a 100mm dish of HUVEC, appropriate amount of virus was determined (number of endothelial cells)(MOI)/(pfu/ml), and was subsequently diluted to 200µl of PBS^{++}, adsorbed at 37°C for 1 hour, with rocking every 15 minutes, followed by addition of 6ml of EGM-2 and incubated overnight at 37°C for further analysis.

Transfection for generation of retroviral vectors. Amphotropic PT67 retroviral packaging cells were seeded at $1*10^5$ cells/well in a 12 well plate and

grown to 90% confluency. One μg of each mutated plasmid DNA was diluted in 50μl of serum-free Dulbecco's Modified Eagle Medium (DMEM, Invitrogen), and 1μl Lipofectamine 2000 Reagent (Life Technologies, Rockville, MD) was diluted in 50μl of serum-free DMEM and incubated at room temperature for 5 min. Subsequently, the two solutions were then mixed together and the mixture was incubated at room temperature for a further 20 min. 100μl of the mixture was then added to each well and cells were then incubated at 37°C. After 48 hours, the cells were put under selection by addition of 400μg/ml of Geneticin (Gibco) to the growth medium. The media was changed every 48 hours and the resistant clones that integrated the neomycin resistance gene from incorporation of the transfected plasmid DNA were isolated and expanded. To isolate retroviral vectors, cells were grown to confluence, placed in normal growth media (no Geneticin), and supernatants containing the produced retroviruses were collected after 24 hours, supplemented with 10% glycerol and frozen at –80°C for storage.

Infection of Cells with Retroviral Vectors. HDMEC were seeded at $1*10^5$ cells/well in 6 well plates, and grown to 80% confluency. Retroviral supernatants were thawed and mixed with 4μg/ml Polybrene (hexadimethrine bromide, Sigma), and filtered through a 0.45μm filter. A 400μl aliquot of prepared supernatant was placed in each well, and after a 2 hour incubation period to allow viral adsorption, 2ml of EGM-2MV growth media was added to each well. The infection step was repeated the next day to increase the efficiency of retroviral infection. Infected cells were cultured for an additional 48 hours and subsequently were put under selection with 200μg/ml of Geneticin in EGM-2MV media to isolate resistant cell clones that

carried the retroviral vector insert. Resistant clones were expanded into 60mm plates and seeded on coverslips for immunocytochemical detection.

Western blotting. Following seeding and stimulation for various periods of time, endothelial cells were scraped and lysed in FRAK's buffer. Lysates were collected in microfuge tubes and passed through a 26 gauge needle several times to reduce viscosity followed by centrifugation at 18,000g at 4°C in a microfuge to remove insoluble material. Supernatants were transferred to new tubes, and the protein concentration of each lysate was subsequently determined using the BCA (bicinchoninic acid) kit according to the manufacturer's directions (Pierce, Rockford, IL). A 30μg quantity of total protein was diluted in SDS-PAGE (sodium dodecyl sulfate polyacrylamide gel electrophoresis) loading buffer (125mM Tris, 4% SDS, 30% glycerol, 2% β-mercaptoethanol), boiled for 5 minutes and loaded on 12% poly-acrylamide gels and subsequently subjected to electrophoresis at 120V followed by transfer to 0.2μm nitrocellulose membranes (Bio-Rad, Hercules, CA) following electrophoresis at 30V overnight at 4°C. Non-specific binding sites on membranes were blocked for 1 hour at room temperature using 5% milk powder in TBST (10mM Tris, 150mM NaCl, 0.5% Tween-20) with the exception of western blots using the ephrinB2 antibody, where 4% casein in TBST was used for blocking. All primary antibodies used for western blot detection were diluted in 5% milk powder in TBST and incubated on the membranes for 1 hour at room temperature, with the exception of antibody for ephrinB2 where 1% bovine serum albumin (BSA) in TBST was used as a diluent and membranes were incubated overnight at 4°C. Following incubation with primary antibody, membranes were washed 4 times for 5 minutes each time with

TBST prior to incubation with secondary antibody. Secondary antibodies were diluted in 5% powdered milk in TBST and incubated with membranes for 1 hour at room temperature, with the exception of the anti-goat-HRP, which was diluted in 1% BSA in TBST, followed by washing 4 times by 5 minutes each time with TBST. Detection of bound antibodies was performed following incubation of membranes with an enhanced chemiluminescence solution (Supersignal, Pierce, Rockford, IL) for 5 min and exposure to Kodak X-Omat film, or alternatively were detected using a Gene Gnome gel documentation system (Syngene, Frederick, MD).

Extracellular Matrix (ECM) coating. Tissue culture plates were coated with a variety of extracellular matrix proteins as follows:

Collagen I: Collagen (Vitrogen 100, Cohesion Technologies, Palo Alto, CA) was diluted in 0.01N HCl to a concentration that resulted in 5μg/cm^2 of collagen added to each well or dish. Wells were allowed to air-dry overnight in the fume hood and were ready to be seeded with cells the next day.

Tenascin-C: Tenascin-C (Chemicon, Temecula, CA) was diluted to a concentration of 0.1μg/mL in PBS and added to wells to cover the bottom. Plates were then incubated overnight at 4°C. Wells were blocked the next day with 0.1% casein for 1 hour followed by three washes in PBS prior to seeding with HUVEC.

Fibronectin: Fibronectin (Invitrogen, Burlington, ON) was diluted to a concentration that resulted in 1μg/cm^2 of the matrix added to each well. Plates were incubated at room temperature for at least one hour. Following incubation, the plates were washed once with sterile distilled water before seeding with HUVEC.

Laminin: Laminin (Sigma, St. Louis, MO) was diluted to 1μg/cm^2 in PBS and added to each well followed by air-drying overnight in a fume hood. Plates were then washed with PBS, and HUVEC were seeded the next day.

Vitronectin: Vitronectin (Sigma, St. Louis, MO) was diluted in PBS to 100ng/cm^2 and added to each well. Plates were then incubated for 1-2 hours at 37°C. Plates were washed with PBS and seeded with HUVEC.

Poly-D-lysine: Poly-D-lysine (BD Biosceinces, Franklin Lakes, NJ) was diluted in sterile water at concentration of 0.1mg/ml. 500μl was incubated in each well of a 24-well plate for 5 minutes, washed with sterile water and air-dried for several hours in a fume hood prior to seeding.

Adhesion Assay. HUVEC were infected with adenoviral vectors encoding ephrinB2 or the various mutant versions of ephrinB2, and 24 hours later were removed by incubation with ice-cold 5mM EDTA in PBS so that membrane bound proteins (ephrins) remain undisturbed. Cells were centrifuged at 1,100*g* in a Beckman Avanti centrifuge and resuspended at 200,000 cells/ml in MCDB 131 supplemented with 1% FBS. 100,000 cells were then seeded on 24 well plates coated with the different ECM proteins. Cells were allowed to adhere to the coated dishes for 45 minutes at 37°C and subsequently non-adherent cells were washed off by rinsing two times with HBSS. Attached cells were then collected by trypsinization and diluted in MCDB 131 + 5% FBS and 700μl were counted using Vi-CELL XR cell viability analyzer (Beckman Coulter, Fullerton, CA).

Apoptosis Assay. HDMEC were grown to confluency in EGM-2MV in 60mm dishes and infected with different ephrinB2 mutant adenoviral vectors or a control

adenoviral vector at different MOI. After 24 or 48 hours, the cell supernatant containing floating cells was collected along with two washes and the attached cells were then isolated following trypsinization and pooled with the media and washes. Cells were kept on ice at all stages. Samples were centrifuged at 1100*g* for 5 minutes followed by two washes of the pellet with ice-cold PBS. Pellets were resuspended in 70% ethanol and incubated a minimum of 20 hours at -20°C to permeabilize the cells. Cells were then washed 2 times with PBS and resuspended in PBS containing 100μg/mL propidium iodide and 40μg/mL RNAse A (both from Sigma), followed by incubation at 4°C for 30 minutes. Samples were then analyzed using a Becton Dickinson LSR Flow Cytometer (BD, Franklin Lakes, NJ) on the FL-2 laser and the sub-G1 population was recorded. The sub-G1 population is defined by having less DNA (ie, fluourescence) than a diploid cell and is characteristic of fragmented DNA as seen during apoptosis. Uninfected cells were analyzed to determine the basal level of apoptosis and the percentage of sub-G1 cells in each sample was compared to the percentage of sub-G1 cells in this population.

Wounding Assay. HUVEC were grown to confluency in 6-well plates or in 6-well plates on glass coverslips in EGM-2. For overexpression of proteins, cells were infected with adenoviral vectors 24 hours prior to wounding. Using a sterile P200 pipette tip, a uniform scrape (wound) was made through the cell monolayer. Scraped cells were washed off using HBSS, and MCDB 131 supplemented with 5% FBS alone or with 50ng/ml VEGF was added. Cells were examined every 24 hours and a digital image was taken with a Nikon CoolPix5400 digital camera mounted to a Nikon Eclipse TE2000 U microscope (Nikon, Toronto, ON) at 40x magnification at 6

points along the wound. Cells were also fixed at various times points during the experiment with 4% paraformaldehyde, and subsequently stained for ephrinB2 expression using immunoflourescent detection methods. Digital images were analyzed and the distances between the two closest cells in the wound were measured, and compared to the original wound distance. The initial average wound size at time 0 was determined and used to subsequently calculate the percent closure over time for each sample.

Immunofluorescence Staining. Endothelial cells were seeded onto sterile glass cover slips in 6-well plates and grown to confluency. Cells were then either left uninfected and processed, or infected with adenoviral vectors and processed 24 hours later. Cells were washed twice (5 minutes each time) with PBS prior to fixation with 4% paraformaldehyde (Sigma) in PBS for 20 min. Following fixation, cells were washed twice with PBS and permeabilized with PBS supplemented with 0.2% Triton X-100 and 1% BSA for 20 min. Cells were then washed twice with PBS, and non-specific binding sites were blocked following incubation for 1 hour in PBS supplemented with 1% BSA and 5% chicken serum. Cells were subsequently incubated with 1:50 anti-ephrinB2 (R&D Systems), or 1:50 anti-Rho (Santa Cruz) primary antibodies diluted in PBS supplemented with 1% BSA overnight at 4°C. Following incubation, cells were washed three times by 5 minutes each time with PBS, followed by incubation with 4μg/ml AlexaFluor-488 conjugated chicken anti-goat IgG (Molecular Probes, Eugene, OR) together with 6.6μM TRITC-conjugated phalloidin (Sigma) and 1μg/ml Hoechst No 33258 (bis-benzamide, Sigma) in PBS with 1% BSA for 2 hours at room temperature in the dark to visualize ephrinB2 (or

Rho), actin cytoskeleton, and nucleus respectively. Cells were then washed three times with PBS in the dark and the slides were subsequently air-dried. Cover slips were then mounted on glass slides using fluorescent mounting media (KPL, Columbia, MD), and sealed with nail polish. The fluorescent images were obtained using an epifluorescent microscope Axioscope 2 (Zeiss, Toronto, ON) at 400X and 1000X magnifications using Dapi filter for Hoechst, Cy3 filter for phalloidin and FITC filter for ephrinB2 or Rho.

Rac GTPase Activity Assay: Generation of GST-PAK and GST-C21.

Plasmids expressing GST-PAK and GST-C21 were obtained from Dr. John G. Collard of the Netherlands Cancer Institute. BL-21(DE3)P-lys-S bacterial cells were transformed with the GST-PAK and GST-C21 plasmids and a stock of transformed cells was frozen in LB with 10% glycerol at -80°C. To propagate the plasmids, 30ml of LB medium containing 100μg/ml ampicillin were inoculated with the glycerol bacterial stock and grown overnight at 37°C. The overnight culture was used to inoculate 1L of LB medium (containing100μg/ml ampicillin) which was then incubated for 3 hours at 37°C. Transcription of the plasmid-encoded proteins was then induced by adding 0.8mM isopropyl-D-thiogalactopyranoside (IPTG) followed by incubation for 3 hours at 30°C. The bacterial suspension was then centrifuged for 10 minutes at 5000g and resuspended in 10ml of bacterial lysis buffer (50mM Tris-HCl pH 7.5, 150mM NaCl, 5mM $MgCl_2$, 1mM dithothreitol, 1mM EDTA, 1mM phenylmethylsulfonylfluoride, 1μg/ml lysozyme, 20μg/ml DNAseI, and 1μg/ml aprotinin). The *E.coli* lysate was incubated 30 minutes on ice, sonicated and centrifuged for 10 min at 10,000g at 4°C. The fusion protein was purified from the

supernatant with glutathione-sepharose 4B beads (Amersham Biosciences, Uppsala, Sweden) previously washed 5 times in bacterial lysis buffer. Briefly, a 1ml aliquot of 50% Glutathione-sepharose bead slurry was incubated with the lysate for 2 hours at 4°C, centrifuged 5 minutes at 2000g at 4°C, and washed 5 times with bacterial washing buffer (50mM Tris-HCl pH 8.0, 150mM NaCl, 5mM $MgCl_2$, 1mM dithothreitol, 1mM phenylmethylsulfonylfluoride, and 1μg/ml aprotinin). Beads were aliquoted in washing buffer containing 10% glycerol, and stored at -80°C until further use in Rho or Rac activation assays.

Rac activation. HUVEC were grown to confluence and infected with adenovirus expressing ephrinB2, control adenovirus vector AdDC315, or were mock infected with PBS^{++}. Following incubation at 37°C for 24 hours, cells were washed twice with HBSS, and serum starved with unsupplemented MCDB 131 overnight. Cells were then stimulated with 0.01μg/ml, 0.1μg/ml, and 1.0μg/ml of EphB6-Fc, 100ng/ml EGF (as a positive control) or human IgG as a negative control for 30 minutes. Cells were washed with cold PBS, and lysed with cold lysis buffer (50mM Tris-HCl pH 7.5, 200mM NaCl, 10mM $MgCl_2$, 1% Nonident P-40, 5% glycerol, 1mM phenylmethylsulfonylfluoride, 1μg/ml leupeptin, and 1μg/ml aprotinin). The resulting cell lysates were kept on ice for 5 minutes then clarified by centrifugation at 4°C for 10 minutes at 10,000g on a table-top centrifuge. Protein concentrations were quantified using the BioRad (Bradford-based) Protein Assay (BioRad, Mississauga, ON). For a positive control, 100μl of cell lysate was mixed with 12μl of 0.2M EDTA and 12μl of 1mM GTPγS (Upstate, Lake Placid, NY) and incubated 10 minutes at 30°C to load the GTP sites. The exchange reaction was stopped by the addition of

8μl of 1M $MgCl_2$. For the affinity precipitation assay, 800μg of protein diluted in lysis buffer was incubated with 50μl of GST-PAK bound bead slurry for 1 hour at 4°C, centrifuged 2 minutes at 2000g at 4°C, and washed 3 times with washing buffer (25mM Tris-HCl pH 7.6, 40mM NaCl, 30mM $MgCl_2$, 1% Nonident P-40, 1mM dithothreitol, 1mM phenylmethylsulfonylfluoride, 1μg/ml leupeptin, and 1μg/ml aprotinin), and two times with the same buffer without added Nonident P-40. The bead pellet was resuspended in 4X Laemmli sample buffer (50mM Tris-HCl pH 6.8, 10 % glycerol, 2% SDS, 2% β-mercaptoethanol, 1% bromophenol blue), boiled for 5 minutes and separated on 4-12% NuPAGE Bis-Tris pre-cast gels (Invitrogen), transferred onto nitrocellulose membrane and blotted with anti-Rac antibody as described above (Upstate, Lake Placid, NY). Densitometry analysis was performed using GeneTools, version 3.06 (SynGene, Cambridge, England)

F-actin/G-actin staining. HUVEC were grown to confluence and infected with different adenoviral vectors, and 24 hours post-infection, cells were washed twice with HBSS, and trypsinized. Cells were collected by centrifugation at 1100g at 4°C, and the pellets were then washed twice with PBS. Cells were then fixed with 4% paraformaldehyde in PBS for 20 minutes, and washed twice with PBS, followed by permeabilization with 0.1% Triton X-100 in PBS + 1% BSA for 20 minutes. Cells were subsequently washed twice and stained with either 6.6μM Alexa Fluor-488-conjugated phalloidin in PBS + 1% BSA or 0.3μM Alexa Fluor-488-conjugated DNase I in PBS + 1% BSA for 20 minutes at room temperature in the dark to stain the F-actin and G-actin respectively. Cells were once again washed twice in PBS and

resuspended in 1ml of PBS followed by analysis on FL1 channel using the Beckman Epics XL flow cytometer (Beckman Coulter, Fullerton, CA).

Statistics. An unpaired t-test was performed using StatView, version 5.0.1 (SAS Institute, Cary, NC).

Results

Our laboratory initially began to examine the potential role of ephrin-Eph receptor interactions in tumour associated angiogenesis and tumour progression and metastasis by determining which family members were expressed in human dermal microvascular endothelial cells (HDMEC) by RT-PCR using RNA isolated from HDMEC that were either cultured in the regular medium, or medium supplemented with 50ng/ml of the angiogenic factor VEGF. It was found that HDMEC express varying levels of EphB1, B2 and B4, and no detectable expression of EphB6. It was also found that they express high levels of ephrinB1 and moderate levels of ephrinB2. Additionally, it was found that VEGF stimulation resulted in an increase in ephrinB2 expression in HDMEC, while VEGF stimulation had no effect on the levels of expression of any of the other detectable ephrin or EphB receptors. This increase in ephrinB2 expression was even more evident in the VEGF-stimulated HDMEC grown on collagenI for 9 days that are forming tube-like structures indicative of sprouting. The upregulation of the ephrinB2 ligand in response to VEGF stimulation was also observed at the protein level. Since VEGF is a very potent angiogenic factor, we decided to further examine the potential role of ephrinB2 in the process of VEGF-induced angiogenesis.

For initial experiments, human dermal microvascular endothelial cells (HDMEC) that were isolated from dermal capillaries were used. HDMEC are a primary cell line and have a population doubling time of approximately 32 hours in

endothelial growth medium (according to manufacturer's product information). Their normal turnover in the body is hundreds of days, however, it can increase to approximately every five days during active remodeling of vasculature (Folkman and D'Amore, 1996). These cells more closely imitate the range of capillary venous and arterial endothelial cells that are recruited by the tumour in its normal environment. However, due to slow growth, lot-to-lot variation of the behavior of these primary cells, and difficulties in culturing, we decided to switch to human umbilical vein endothelial cells (HUVEC). HUVEC are large vessel cells that are lacking an arterial supply of endothelial cells. Even though there have been biological differences reported in the responses of HDMEC and HUVEC to chemokine receptors (Salceto et al, 2000), we believe that basic signal transduction through ephrinB signaling is the same or similar in the two cell types. We have thus used both cell lines to examine the ephrinB2 reverse signaling in endothelial cells, and how it affects their migration and actin cytoskeleton remodeling.

1. Endogenous Expression of EphrinB2

Initial experiments showing that VEGF stimulation resulted in an increase in ephrinB2 expression in HDMEC was repeated, and indeed, it was found that there was a dose dependent increase of ephrinB2 expression at the message level by RT-PCR following 48 hour stimulation with varying doses of VEGF (Figure 3). It is worth mentioning that the band representing ephrinB2 in the unstimulated HDMEC condition appears to be darker than that observed following stimulation with 2ng/ml VEGF. However, it must be noted that PCR is only semi-quantitative and not as reliable as real-time quantitative PCR. Therefore, this could be an artifact of amplification. Nevertheless, a clear increase in ephrinB2 mRNA levels can be seen with increasing concentrations of VEGF-stimulation. This increase in ephrinB2 expression was also observed in HUVEC treated in a similar fashion (Figure 4). As seen in Figure 4, ephrinB2 levels increased in response to VEGF stimulation, and this effect was observed as early as 24 hours post stimulation, but was not seen at either 2 or 8 hours post stimulation (data not shown). The primers to amplify ephrinB2 mRNA were designed to be exon spanning, therefore any contamination with genomic DNA would result in a fragment with a much larger size than expected. No such bands were observed under any of the conditions tested, thus we can be sure that the PCR products obtained are a result of amplification of mRNA in our lysates. The upregulation of the ephrinB2 ligand in response to VEGF stimulation was also observed at the protein level (Figure 5). It is interesting to note that only VEGF stimulation showed a dose-dependent change in ephrinB2 levels, while no such effect

was observed following stimulation with other angiogenic factors like EGF and bFGF. There was however an increase in ephrinB2 expression following EGF and bFGF stimulation as compared to unstimulated control cells, however we did not observe further increases in expression with increasing doses of these growth factors. Since VEGF is a very potent angiogenic factor, we decided to further examine the potential role of ephrinB2 in the process of VEGF-induced angiogenesis. Since we confirmed that there are no major differences between the two endothelial cell types, at least with respect to VEGF induced ephrinB2 regulation, it seemed reasonable to pursue our studies using HUVEC.

Figure 3. VEGF induces ephrinB2 expression in HDMEC. HDMEC were treated with 2ng/ml, 10ng/ml, 50ng/ml, or 250ng/ml of VEGF for 48 hours. Cells were then lysed with TRIzol reagent and total RNA was isolated. Following reverse transcription using oligo-dT as a primer, the ephrinB2 gene was amplified using specific primers as described in the materials and methods. Expression of GAPDH was used as a control to ensure equal amounts of RNA template were used in each reaction. Non-reverse transcribed RNA (No-RT) was also used as a negative control. Expression of ephrinB2 was observed to increase with increasing concentrations of VEGF.

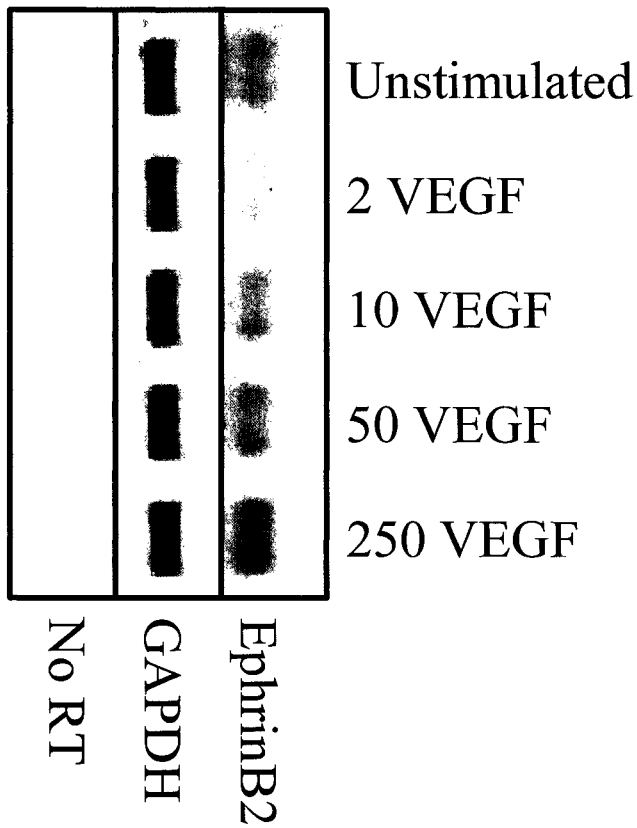
Unstimulated
2 VEGF
10 VEGF
50 VEGF
250 VEGF
No RT
GAPDH
EphrinB2

Figure 4. VEGF induces ephrinB2 expression in HUVEC. HUVEC were treated with 10ng/ml, 50ng/ml, or 250ng/ml of VEGF for 24 or 48 hours. Cells were then lysed with TRIzol reagent and total RNA was isolated. Following reverse transcription using oligo-dT as a primer, the ephrinB2 gene was amplified using specific primers as described in the materials and methods. Expression of GAPDH was used as a control to ensure equal amounts of RNA template were used in each reaction. Expression of ephrinB2 was observed to increase with increasing concentrations of VEGF.

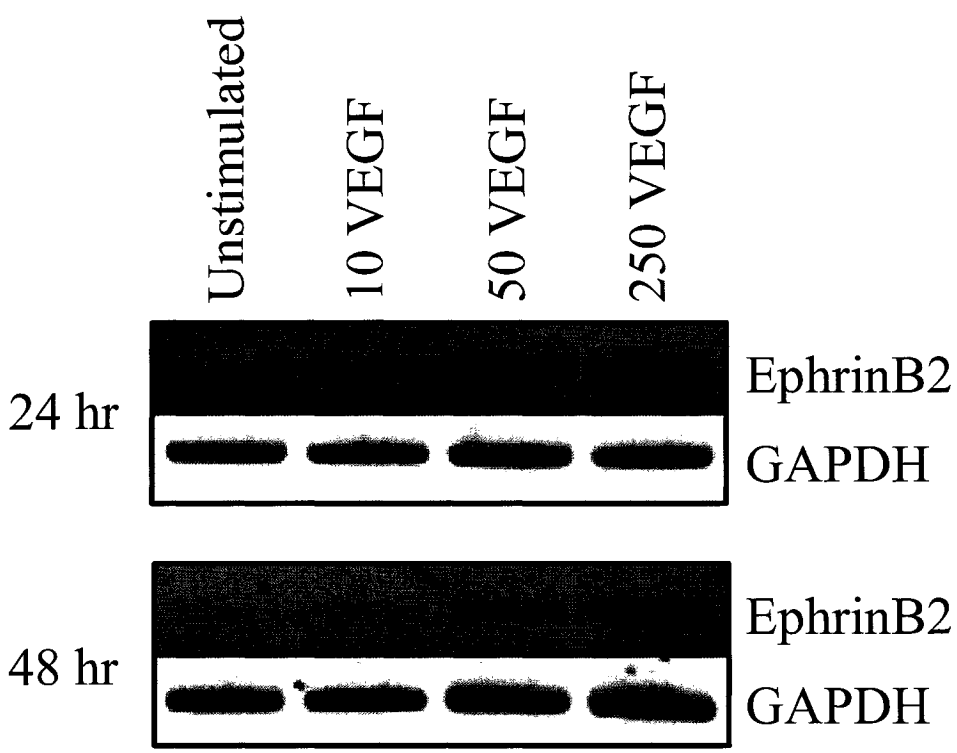
Unstimulated
10 VEGF
50 VEGF
250 VEGF
24 hr
EphrinB2
GAPDH
48 hr
EphrinB2
GAPDH

Figure 5. VEGF-induced increase in ephrinB2 expression is observed at the protein level. HUVEC were treated with 10ng/ml, 50ng/ml, or 250ng/ml of VEGF, 1ng/ml, 10ng/ml, or 50ng/ml of EGF, and 10ng/ml, 50ng/ml, or 250ng/ml of bFGF for 24 hours. Cells were then lysed followed by western blot detection of ephrinB2 expression as described in materials and methods. Anti-tubulin antibody was used as a loading control to ensure equal protein concentrations in each sample. EphrinB2 levels increase with increasing doses of VEGF stimulation, and besides an initial increase as compared to unstimulated controls, no dose-dependent changes were observed in EGF and bFGF stimulated cells.

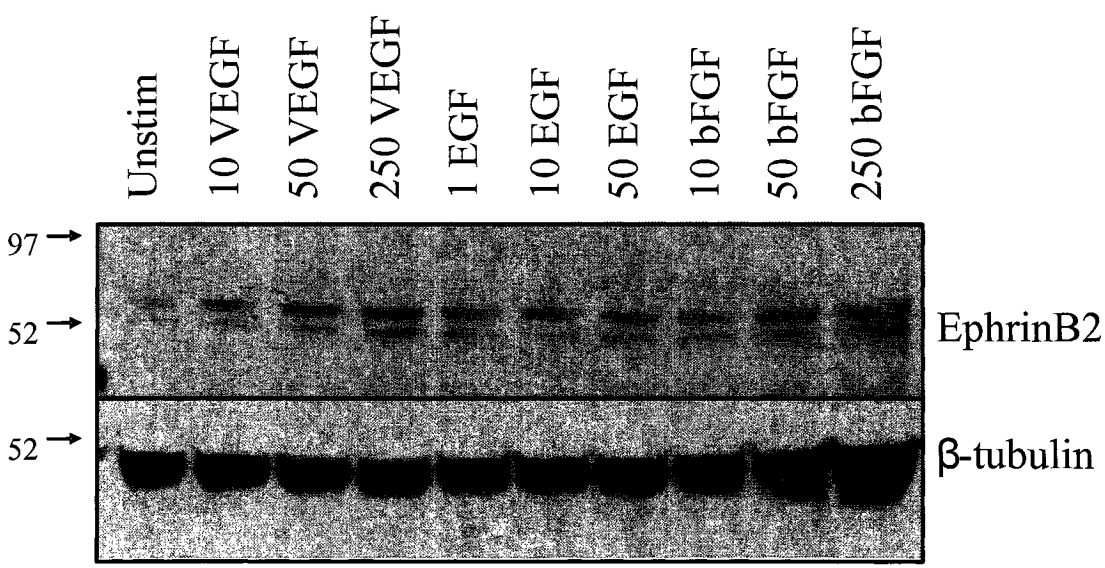
Unstim
10 VEGF
50 VEGF
250 VEGF
1 EGF
10 EGF
50 EGF
10 bFGF
50 bFGF
250 bFGF
97
52
52
EphrinB2
β-tubulin

2. Mutagenesis and Overexpression

In order to characterize the role of ephrinB2 mediated reverse signaling in angiogenesis, tyrosine residues that might serve as potential phosphorylation sites in the cytoplasmic tail of ephrinB2 were mutated to phenylalanine. Phenylalanine was chosen because this amino acid residue most closely resembles tyrosine, in that they both have a phenyl group as an R group with the exception of the presence of alcohol group on the tyrosine residue, which renders it phosphorylatable, and the absence of this group in phenylalanine rendering unphosphorylatable. Therefore, by using this conservative amino acid substitution, we minimize any structural change of the entire protein. The individual mutations, as described below, were used to characterize the phenotypic changes that resulted when the mutations were expressed. The specific changes that were noted concerned the ability of the cell to migrate, survive, proliferate, and change shape.

Dr. Christina Addison previously cloned the ephrinB2 cDNA into the retroviral plasmid system pLXSN, to generate pLXSN-EFNB2. This plasmid was subsequently used for all mutagenesis experiments. There are five tyrosines in the cytoplasmic tail of ephrinB2 believed to be potential phosphorylation sites, and all five were mutated to phenylalanine, individually, by site directed mutagenesis using the QuickChange kit from Stratagene (See materials and methods). Specific oligomer primers were designed (See materials and methods) that introduced a single nucleotide change in the parental plasmid. In this case, the mutation involved a single nucleotide change from A to T resulting in a triplet codon change from TAC to TTC,

or GTA to GAA when sequenced from the cytoplasmic tail (reverse) or 3' end of the cDNA (carboxy terminal side of the protein). TAC is the codon encoding tyrosine and TTC is the codon encoding phenylalanine. Furthermore, In addition to individual mutations, which can be used to identify specific interactions within the signaling pathway, a mutant with all tyrosines mutated to phenylalanine was generated to obtain a "signaling dead" control. EphrinB2$_{(Y\text{-}304,311,316,330,331\text{-}F)}$ was generated by introducing one mutation at a time and using previously mutated plasmid as a template. All mutations were confirmed by sequencing to ensure the appropriate point mutation had occurred (Figure 6).

Wildtype and mutant LXSN-EFNB2 plasmids were transfected into the amphotropic retroviral packaging PT67 cell line and Geneticin resistant colonies were expanded. PT67 cells were lysed and total protein extracts were probed for ephrinB2 expression (Figure 7). Transfection of PT67 cells with the pLXSN-EFNB2 plasmid led to a significant increase in ephrinB2 levels. Supernatants from PT67 stably transduced expressing cell lines were used to subsequently infect HDMEC. We used a retroviral-based transfection method for our experiments as it has been previously observed that HDMEC are difficult to transfect using common lipid-based transfection agents. Following the selection of Geneticin-resistant HDMEC, ephrinB2 expressing or control LXSN infected cells were seeded onto cover slips and subsequently fixed, permeabilized and stained with FITC-conjugated phalloidin to visualize the cytoskeleton (Figure 8). As can be seen in Figure 8, control HDMEC are slightly elongated cells with actin filaments that run the length of the cell in a parallel fashion. In contrast, ephrinB2 overexpressing HDMEC have irregular shape,

and very disorganized actin filaments that often run perpendicular to one another and appear to be more cross-linked than in control HDMEC. Overexpression of mutant versions of ephrinB2 (that have a single tyrosine site changed to a phenylalanine) in HDMEC led to an even more dramatic rearrangement of the actin cytoskeleton. Every mutation seemed to have its own unique phenotype, however ephrinB2$_{(Y316F)}$ overexpression had the most striking effects on actin cytoskeleton, with actin stress fibers being very clustered and cross-linked at few points throughout the cell. The phenotype was also characterized by round cellular shape and no contact with other cells. Furthermore, ephrinB2$_{(Y311F)}$ overexpression most closely resembled the phenotype of the wildtype eprhinB2 overexpressing cells, with irregular shape and apparent cross-linked actin filaments. These cells also lacked contact with other cells. And lastly, overexpression of two mutant ephrinB2 proteins, ephrinB2$_{(Y330F)}$ and ephrinB2$_{(Y331F)}$ which comprise the PDZ binding domain, resulted in a similar phenotype, where cells appeared more rounded however remained in contact with each other. Their actin cytoskeleton did not appear to be disorganized, but appeared to have reduced stress fiber formation normally seen spanning the length of the cell. This effect is particularly noticeable in cells with ephrinB2$_{(Y330F)}$ overexpression.

A common characteristic of all ephrinB2 stably overexpressing cells generated by retroviral transduction was that the cells proliferated at extremely low rates as compared to control retroviral transduced cells. For example, cells were passaged into larger tissue culture dishes once every 3-4 weeks as compared to once a week for control transduced cells (data not shown). Due to a lack of proliferation, we could never obtain enough cells to perform further characterization experiments.

Since the slow proliferation rate of ephrinB2 transduced cells, combined with low doubling times of primary cells impaired our ability to expand the cells to sufficient numbers to perform additional experiments, we chose to use another strategy of overexpressing ephrinB2 using adenoviral vector infection. Despite the inhibitory effects of HDMEC proliferation, we observed dramatic changes on the cell cytoskeleton following retroviral transduction suggesting that ephrinB2 overexpression and signaling alters the cytoskeleton phenotype in HDMEC and may play a role in endothelial cell morphology and migration during angiogenesis.

Figure 6. Sequencing results of ephrinB2 mutations. The sequences show the cytoplasmic tail of ephrinB2, as well as overlapping mutagenesis primer sequences in reverse. All tyrosine-to-phenylalanine (GTA to GAA) mutations are underlined and numbered. Correct mutated clones were identified and used for subsequent cloning and vector generation.

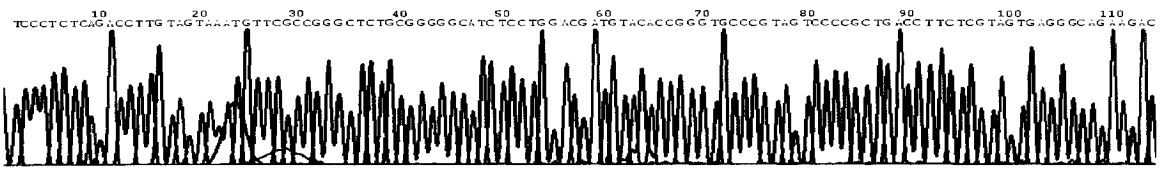

EphrinB2$_{(wt)}$

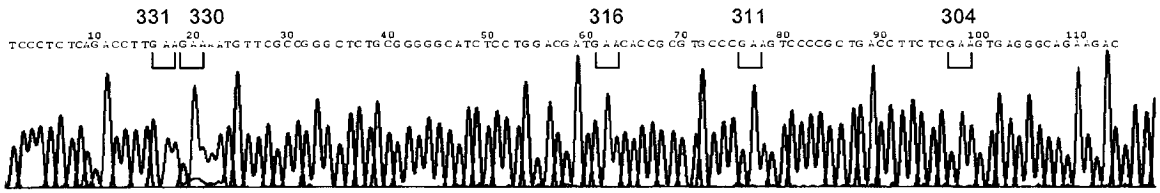

EphrinB2$_{(Y\text{-}304,311,316,330,331\text{-}F)}$

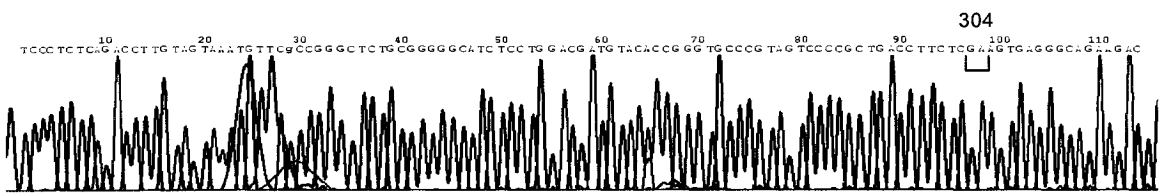

EphrinB2$_{(Y\text{-}304\text{-}F)}$

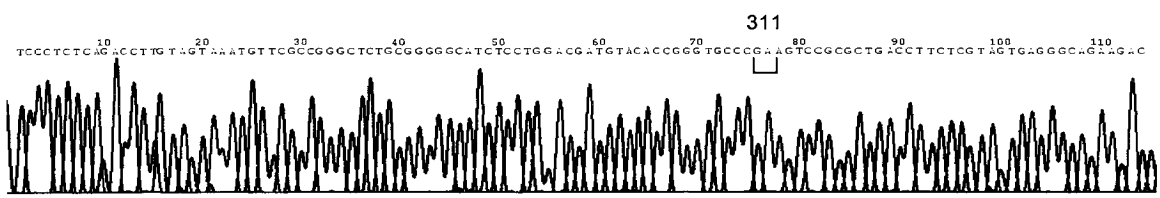

EphrinB2$_{(Y\text{-}311\text{-}F)}$

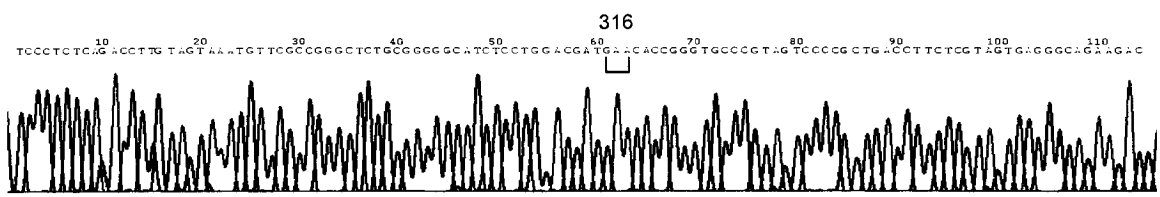

EphrinB2$_{(Y\text{-}316\text{-}F)}$

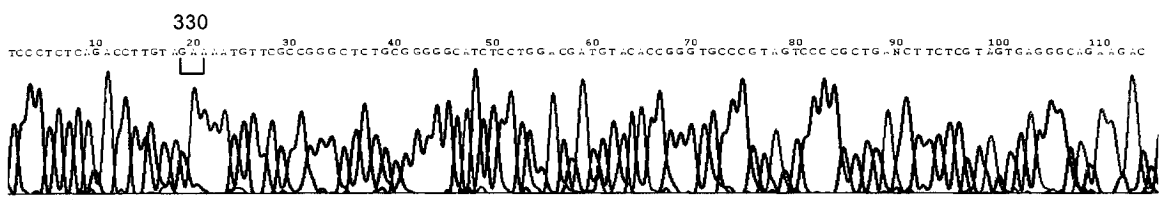

EphrinB2$_{(Y\text{-}330\text{-}F)}$

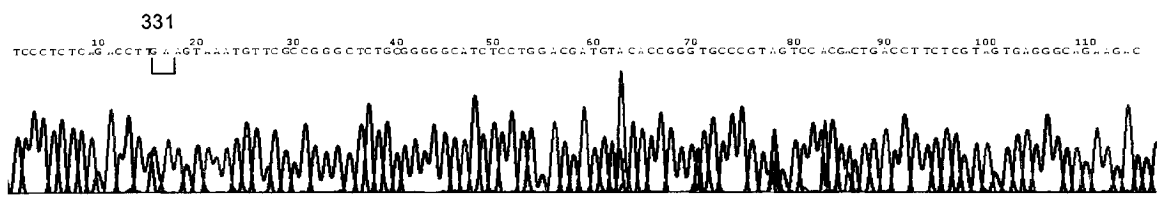

EphrinB2$_{(Y\text{-}331\text{-}F)}$

Figure 7. Overexpression of ephrinB2. PT67 cells were transfected with pLXSN plasmid, and Geneticin resistant colonies were expanded. Cells were lysed to generate total protein extracts which were then subjected to western blot analysis to observe ephrinB2 expression. Anti-tubulin was used as a loading control to ensure equal protein levels. EphrinB2 levels are increased following pLXSN-EFNB2 plasmid transfection.

pLXSN
pLXSN-EFNB2
Ephrin B2
Tubulin

Figure 8. Overexpression of ephrinB2 and the various tyrosine mutants of ephrinB2 caused changes in actin cytoskeleton. HDMEC were infected with control LXSN retrovirus vector, or with retrovirus vectors that overexpress wildtype ephrinB2 or mutant ephrinB2 proteins. Following selection in Geneticin, stably expressing clones were seeded onto glass coverslips and subsequently fixed and permeabilized. Cells were then incubated with TRITC-conjugated Phalloidin to stain the cell F-actin cytoskeleton (red) and Hoechst to visualize the nucleus (blue), and viewed with fluorescent microscope at 400x magnification. Overexpression of ephrinB2 led to modifications of cell shape and actin arrangement within the cells. Scale bars represent 25μm.

LXSN

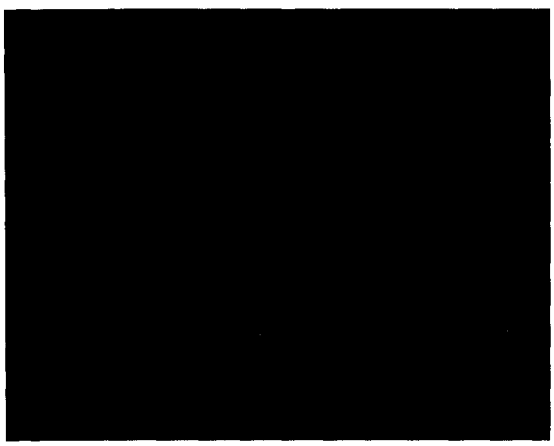

LXSN-EFNB2

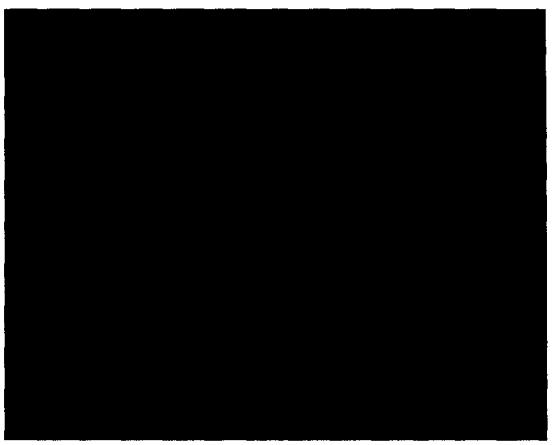

LXSN-EFNB2-Y311F

LXSN-EFNB2-Y316F

LXSN-EFNB2-Y330F

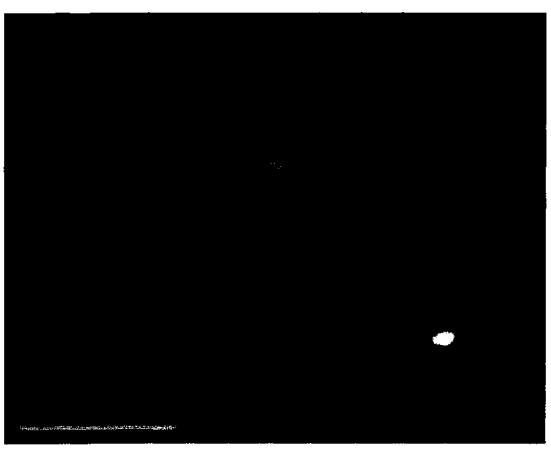

LXSN-EFNB2-Y331F

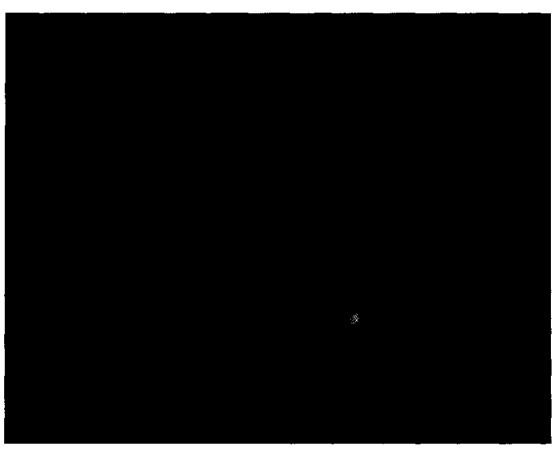

3. Adenoviral Generation and Characterization

As previously mentioned, HDMEC overexpressing ephrinB2 or any of its mutated forms by retroviral transduction, failed to adequately proliferate to yield enough cells to perform various experiments that would elucidate the role of ephrinB2 reverse signaling. Therefore, we decided to generate adenoviral vectors that express ephrinB2 and its various mutants, in order to transiently infect confluent endothelial cells and subsequently perform characterization experiments. EphrinB2 cDNAs, wildtype as well as mutants, were isolated following amplification by PCR from pLXSN-EFNB2 plasmid (or mutant versions) as a template and using specific primers as described in Materials and Methods. The isolated genes were then purified and cloned into the pDC315 adenoviral shuttle plasmid, which was subsequently used for co-transfection together with pBHGΔE1,3loxP adenoviral genomic plasmid. Following plasmid co-transfection in 293 cells, adenoviral vectors containing the gene of interest were generated by site-specific recombination *in vivo*. Viral plaques were then isolated and the identity of the vectors was confirmed by isolation of viral DNA and restriction enzyme digestion to visualize the predicted DNA structure. Once confirmed, high titer viral stocks were generated and titered as described in Materials and Methods.

High titer viral stocks for wildtype (Ad-EFNB2) and each mutant were used to infect confluent HUVEC at a multiplicity of infection (MOI) of 5, that is, five viral particles per cell. Cells were lysed 24 hours later and total protein extracts were probed for ephrinB2 expression by western blot (Figure 9). As the figure clearly

indicates, ephrinB2 along with mutant ephrinB2 could be overexpressed in infected cells using the adenoviral vector system. Furthermore, we examined if there was a dose-dependent effect on the levels of ephrinB2 overexpression by using different MOI of adenoviral vectors for infection (Figure 10). We observed a dose-dependent increase in the expression of the ephrinB2 transgene following infection using increasing MOI of adenovirus, thus by using this system, we could control how much ephrinB2 cells would overexpress. We also determined the duration of expression of ephrinB2 following adenoviral vector infection of HUVEC (Figure 11). We observed overexpression of ephrinB2 as early as 24 hours post infection, and found expression continued for at least 96 hours post infection, which was the duration of all subsequent experiments. These data suggest that we successfully generated a method by which to highly overexpress ephrinB2 in a large number of cells simultaneously.

One phenomenon that was noticed when endothelial cells were infected with higher doses of adenovirus vectors expressing ephrinB2 was that the cells started to detach from the dish (Figure 12). This was best seen in the cells that were infected with an MOI of 50 or 100 pfu/cell. Mock infected cells, as well as control adenoviral vector, or ephrinB2 infected cell profiles appeared similar when low doses of viral vectors are used, such as an MOI of 1pfu/cell, or 5pfu/cell. However, when a higher dose of ephrinB2 expressing viral vector was used, such as 10pfu/cell or higher, cells began to detach from the dish, and at an MOI of 100pfu/cell, the majority of the cells detached and were floating in the dishes. The fact that the control viral vector did not affect the cell detachment to the same extent, led us to believe that this cell detachment was due to the overexpression of ephrinB2 and its subsequent effects on

the cell cytoskeleton which may affect cell spreading or adhesion to the extracellular matrix. As our previous data showed that high levels of ephrinB2 expression could be achieved using an MOI as low as 5pfu/cell (Figure 10), and we did not observe the problem of cell detachment at this vector dose, we used an MOI of 5pfu/cell for all subsequent experiments.

In order to determine if overexpression of ephrinB2 altered the ability of the cells to attach to substrates, we next performed adhesion assays, and tested the ability of cells to bind to various extracellular matrix proteins upon overexpression of ephrinB2 or its mutant forms (Figure 13). Briefly, cells were infected with the adenoviral vectors expressing ephrinB2 or its mutants, and 24 hours later, cells were lifted off with cold EDTA to maintain the surface proteins intact. Cells were then reseeded into a new dish and 45 minutes later following removal of non-adherent cells, the bound cells were collected by trypsinization and counted as described in Materials and Methods. The percentage of cells infected with the adenoviral vectors were counted following detection of ephrinB2 overexpression by immunofluorescence (Figure 18), and we observed similar proportions of cells being infected (>80%), with the exception of Ad-Y331F, which had a lower percentage of cells being infected and expressing the appropriate construct. As infection with adenoviral vectors is consistent, and the same amount of the virus was used in quantification of efficiency of infection by immunofluorescence as was used in the adhesion assay (MOI of 5pfu/cell for both experiments), we can infer that infection of cells with the viral vectors and subsequent expression of ephrinB2 or its mutant forms was similar in all cases with the exception of Ad-Y331F. It was found that cells that

overexpress wildtype ephrinB2 have a significant reduction ($p<0.05$) in the number of attached cells to the dish in this short adhesion assay as compared to control infected cells. It was also found that cells overexpressing ephrinB2$_{(Y304F)}$, ephrinB2$_{(Y311F)}$, and ephrinB2$_{(Y330F)}$ had significantly reduced adhesion as compared to the control DC315 infected cells ($p<0.05$). It is also interesting to note that ephrinB2$_{(Y330F)}$ infected cells had significantly higher adhesion compared to the wildtype ephrinB2 infected cells ($p<0.05$), but still somewhat reduced adhesion as compared to control DC315 infected cells. Although there was a slight reduction in adhesion of the ephrinB2$_{(Y316)}$ and ephrinB2$_{(Y331)}$ overexpressing cells, their adherence to substrate was not significantly different then that of control infected cells. This experiment was also performed by seeding the cells onto dishes covered with different extracellular matrices including collagen I, fibronectin, laminin, poly-D-lysine and vitronectin. The same overall pattern of adhesion was observed in all experiments (data not shown), suggesting that this is a general phenomenon and not specific to adhesion to particular substrates. These data suggest that the overexpression of ephrinB2 reduces the attachment of the cells to the matrix, however, mutation of Y330F in the cytoplasmic tail of ephrinB2 can reduce this effect to some extent. The fact that the Y316 and Y331 mutant ephrinB2 proteins were not impaired in adhesion suggests that these particular tyrosine residues may play an important role in the inhibition of cell adhesion by ephrinB2 overexpression.

The fact that we observed an ephrinB2 dependent detachment of cells at higher MOI of adenoviral infection led us to believe that the cells may be dying by the process of anoikis, or programmed cell death due to detachment from the matrix.

The impaired ability to attach to matrix as noted in the adhesion assay would support this contention. As a confirmation, we decided to assay the infected cells for the presence of fragmented DNA (sub-G1) as an indication of apoptosis following staining of permeabilized cells with propidium iodide (Figure 14). Cell debris was gated out upon analysis, therefore figures are representations of the DNA content in intact or apoptotic cells. We found that there were no changes in the distribution of cells in the cell cycle, nor in the number of apoptotic cells following infection with control adenoviral vector DC315 as compared to uninfected cells (Figure 14). However, when ephirnB2 wildtype was expressed, there seemed to be a small increase in sub-G1 population of cells, but this could be due to the shift of the entire peak to the left, compared to the uninfected cells, and not due to the increase of the number of apoptotic cells. It is interesting to note the presence of a third peak to the left of the G1 peak in cells overexpressing mutant ephrinB2. This peak, because it overlaps with the sub-G1 population of cells, appears to increase the number of apoptotic cells. While the reasons for this peak shift to the left are unclear, it is possible that it represents cells that have begun to undergo apoptosis that have not continued to fragment their DNA. Although other experiments, including the adhesion assay showed essentially no differences in the ability of ephrinB2$_{(Y316F)}$ expressing cells to adhere as compared to uninfected or control virus infected cells (Figure 13), these assays were performed with equal numbers of viable cells, thus any increases in apoptosis as a result of mutant ephrinB2 overexpression would not be a factor as apoptotic cells would not have been included in these experiments. Thus it remains possible that the overexpression of mutant versions of ephrinB2 could induce

apoptosis of infected cells, without inducing complete fragmentation of DNA. Alternatively, it is possible that the cells have undergone some chromatin remodeling or condensation that would alter their ability to bind propidium iodide thus resulting in a shift of the fluorescent intensity to the left. To investigate these two hypotheses, alternative assays of apoptosis that do not rely on DNA structure, such as AnnexinV staining or alternatively identifying cells that have undergone DNA strand nicking using BrdU-TUNEL staining to confirm truly apoptotic cells could be used. Further experiments are required in order to ascertain the reasons for this peak shift. However, our data with wild-type ephrinB2 overexpression would suggest that the cells are not lifting off the dish due to undergoing apoptosis but that there is some modification in the ability of the cells to attach to the substratum as a result of ephrinB2 overexpression.

Figure 9. EphrinB2 overexpression following infection with Ad-EFNB2 vectors. HUVEC were either mock infected, infected with control viral vector (DC315) or infected with adenoviral vectors expressing ephrinB2 or its mutant versions at an MOI of 5pfu/cell, and 24 hours later total protein extracts were obtained following cell lysis and subjected to western blot analysis to observe ephrinB2 expression as described in Materials and Methods. Anti-tubulin was used as a loading control to ensure equal protein levels. EphrinB2 levels are increased following infection with Ad-EFNB2 or its mutant versions.


Mock infected
Ad - DC315
Ad - EFNB2
Ad - Y304F
Ad - Y311F
Ad - Y316F
Ad - Y330F
Ad - Y331F
Ad – Y all F
β-tubulin
EphrinB2

Figure 10. Dose-dependent expression of ephrinB2 following infection by Ad-EFNB2. HUVEC were either mock infected or infected with adenoviral vectors expressing ephrinB2 at different multiplicities of infection (MOI) of 1, 5, 10, 50, or 100pfu/cell, and 24 hours later cells were lysed and total protein extracts analyzed by western blot for ephrinB2 expression. Anti-tubulin was used as a loading control to ensure equal protein levels. EphrinB2 levels are increased following infection with higher MOI of Ad-EFNB2.

Mock infected
Ad – EFNB2
MOI=1
MOI=5
MOI=10
MOI=50
MOI=100
EphrinB2
β-tubulin

Figure 11. Duration of ephrinB2 expression following Ad-EFNB2 infection. HUVEC were infected with either control adenoviral vector or adenoviral vector expressing ephrinB2 at an MOI of 5pfu/cell, and 24, 48, 72, and 96 hours later cells were lysed and total protein extracts were subjected to western blot analysis to observe the duration of ephrinB2 expression. Anti-tubulin was used as a loading control for total protein levels. Increased ephrinB2 levels are evident by 24 hours post infection and stay elevated for at least 96 hours post infection.

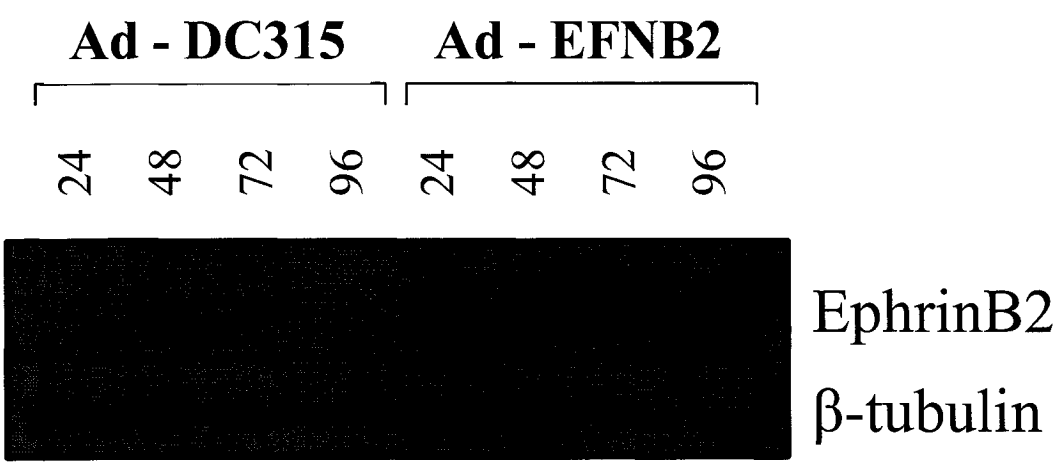
Ad - DC315
Ad - EFNB2
24
48
72
96
24
48
72
96
EphrinB2
β-tubulin

Figure 12. Overexpression of ephrinB2 induces cell detachment at high MOIs. HUVEC were either mock infected, infected with control viral vector DC315, or infected with the adenoviral vector expressing ephrinB2 at MOIs of 1, 5, 10, 50, or 100pfu/cell, and 24 hours later cells were viewed under a microscope at a magnification of 40x. Increased cell detachment was observed following infection of HUVEC with increasing MOIs of Ad-EFNB2.

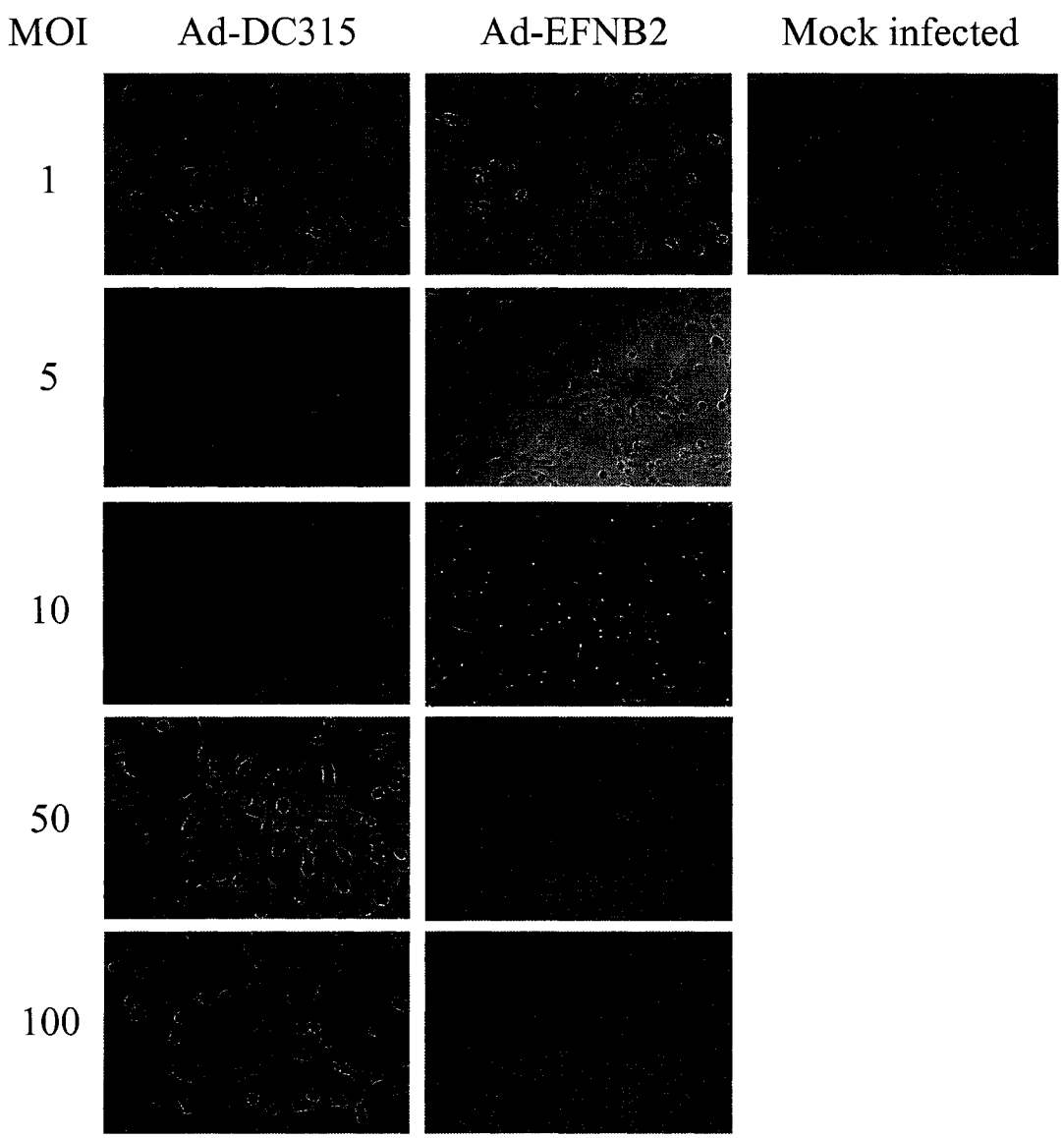
MOI
Ad-DC315
Ad-EFNB2
Mock infected
1
5
10
50
100

Figure 13. Overexpression of ephrinB2 decreases cell adhesion. HUVEC were either mock infected, infected with control viral vector (DC315) or infected with adenoviral vectors expressing ephrinB2 or its mutant versions at an MOI of 5pfu/cell, and 24 hours later cells were removed from the dish with cold EDTA to preserve the surface proteins, and 10^5 cells seeded into new dishes in triplicate. Cells were allowed to adhere for 45 minutes and attached cells were collected and counted as described in Materials and Methods. A p-value <0.05 as compared to the DC315 control infected cells is indicated by the *. EphrinB2 overexpression decreases cell adhesion to the substratum.

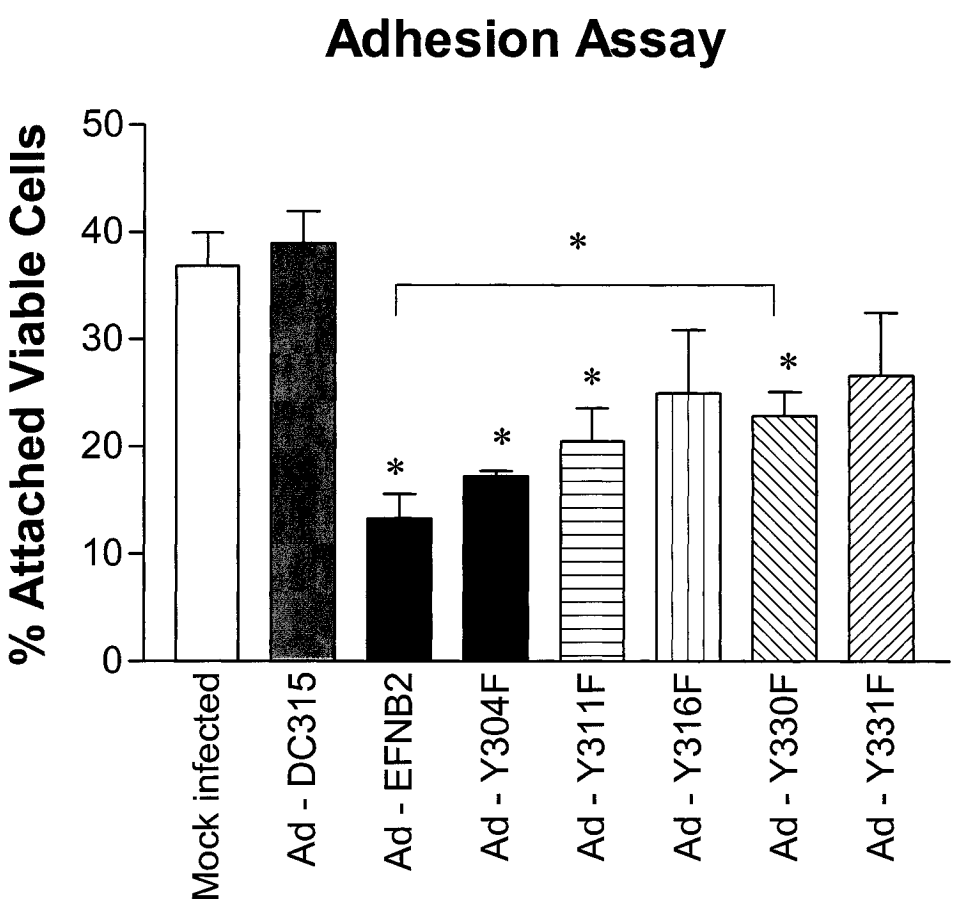
Adhesion Assay
% Attached Viable Cells
50
40
30
20
10
0
*
*
*
*
*
*
Mock infected
Ad - DC315
Ad - EFNB2
Ad - Y304F
Ad - Y311F
Ad - Y316F
Ad - Y330F
Ad - Y331F

Figure 14. Apoptosis assay of infected HUVEC. HUVEC were either mock infected, infected with control adenoviral vector, or adenoviral vectors encoding ephrinB2 and its various mutants, at a MOI of 10, and 24 hours later, floating, as well as attached cells were collected, permeabilized with 70% ethanol and stained with propidium iodide. PI stained cells were then analyzed by flow cytometry on the FL2 channel and the number of cells containing sub-G1 levels of DNA were considered apoptotic.

Uninfected

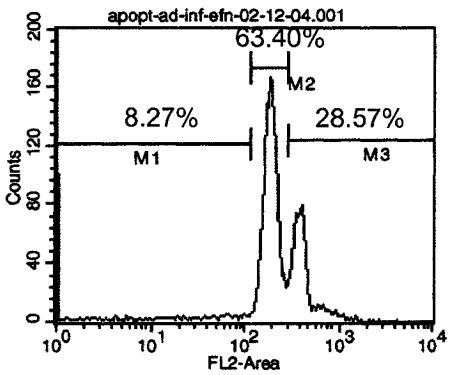

Ad - DC315

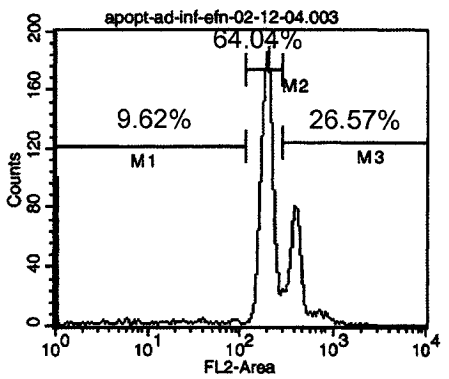

Ad - EFNB2

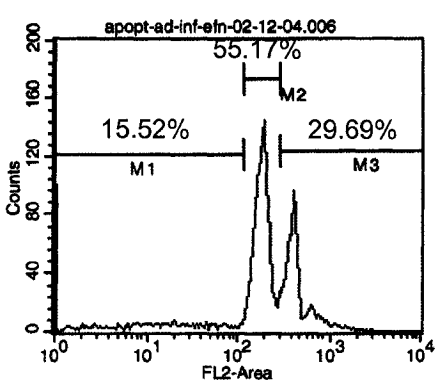

Ad - Y304F

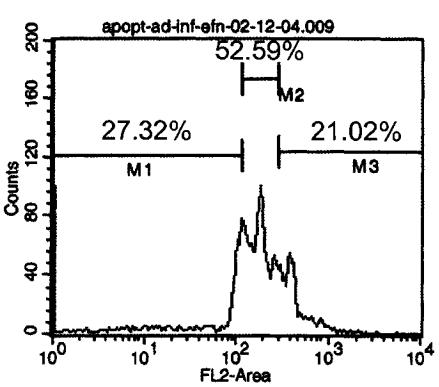

Ad – Y316F

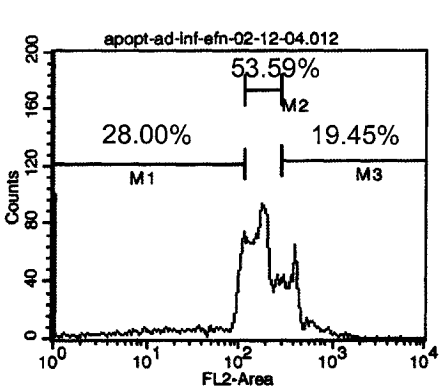

Ad - Y330F

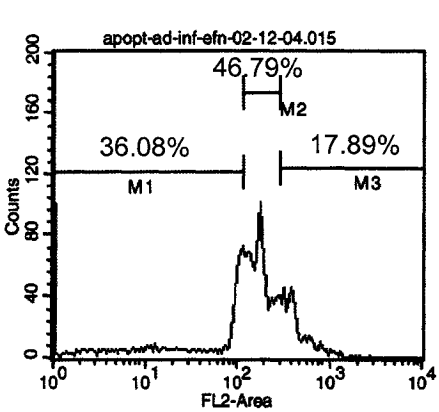

4. Reverse Signaling

It has been previously shown that ephrinB ligands become phosphorylated on tyrosine residues and are involved in bi-directional signaling following binding of their cognate receptors (Cowan and Henkemayer, 2001). Therefore to determine the potential physiological effects of ephrinB2-EphB reverse signaling in endothelial cells, we used the chimeric soluble Eph-Fc receptors to activate the ephrinB2 ligand and thus induce reverse signaling pathways. Eph-Fc receptors are dimeric recombinant molecules and are comprised of the ectodomain of the Eph receptor fused to an IgG-Fc domain, and have been previously shown to be able to bind ephrinB ligands and subsequently induce reverse signaling via phosphorylation of tyrosine residues in the ephrinB cytoplasmic domain (Cowan and Henkemayer, 2001). Multiple receptors have been shown to interact with ephrinB2, including EphB1, EphB2, EphB4, and EphB6, however, EphB6 has been demonstrated to only bind ephrinB2 as a ligand (Munthe et al, 2000), thus by using EphB6-Fc, we can specifically target the reverse signaling induced by binding of ephrinB2.

As our previous results using retroviral vector transduction suggested that ephrinB2 may play a role in the remodeling of the actin cytoskeleton, it was logical to assume that ephrinB2 signaling could affect cell migration. To determine the effects of reverse signaling on endothelial cell migration, HUVEC monolayers were wounded and the rate of wound closure, that is migration of cells into the gap, was monitored following stimulation with EphB6-Fc to induce reverse signaling as compared to control IgG stimulation. We found that the cells treated with VEGF plus

control IgG migrated at the same rate as VEGF only stimulated cells, however, cells that were stimulated with VEGF along with any dose of EphB6-Fc showed significantly slower rates of wound closure ($p<0.05$) as compared to the same doses of IgG stimulated cells at 48 hours after wounding (Figure 15). There was also a significant decrease in rates of wound closure when all EphB6-Fc stimulated cells were compared to VEGF only control ($p<0.05$, not shown in the figure). It is interesting to note that there does not seem to be a dose-dependent response in the inhibition of migration following EphB6-Fc stimulation. This could be due to the saturation of ephrinB2 ligands and sufficient activation of reverse signaling even by the lowest dose of EphB6-Fc used in these experiments. It needs to be proven, however, that the reverse signaling actually occurs in this case. This could be done by stimulating endothelial cells with EphB6-Fc receptors and determining if there is phosphorylation of ephrinB2 cytoplasmic tail. It should be noted that this experiment was attempted numerous times, but proved unsuccessful due to antibodies to phospho-ephrinB2 that were not specific enough. However, there are some promising results by immunoprecipitating ephrinB2 and detecting phosphorylation with PY-20 antibody, but these results are not conclusive enough as of now, and more work needs to be done to confirm these findings.

We next wanted to determine the effects of ephrinB2 overexpression on HUVEC migration. HUVEC were grown to confluency in tissue culture dishes and infected with adenoviral vectors encoding ephrinB2, its mutant versions, or control viral vectors. Cells were subsequently wounded and wound closure was monitored on a daily basis as described. It is interesting to note that cells that overexpressed

wildtype ephrinB2 migrated at the same rate as control DC315 infected cells, suggesting that the overexpression of ephrinB2 had no effect on cell migration (Figure 16). However it is worth noting, that although ephrinB2 is overexpressed in this system, it is possible that the reverse signaling may not be activated. Furthermore, ephrinB2$_{(Y304F)}$ mutant infected cells showed the same phenotype as wildtype. However, ephrinB2$_{(Y316F)}$ migrated significantly more slowly than the wildtype ephrinB2 expressing cells ($p<0.05$) at 72 hours post wounding, and ephrinB2$_{(Y330F)}$ infected cells migrated even more slowly ($p<0.001$). A second set of experiments was performed in the presence of 50ng/ml of VEGF to increase cell survival and stimulate cell migration. Nevertheless, a similar pattern of migration was observed, where migration of ephrinB2$_{(Y316F)}$ and eprinB2$_{(Y330F)}$ infected cells was impeded as compared to the control vector infected or wildtype infected cells. These results suggest that reverse signaling via ephrinB2 plays a role in endothelial cell migration, and that Y316, and Y330 are the most likely candidates to mediate signal transduction leading to migration, as when mutated and unable to be phosphorylated, a delay in migration is observed. This is also consistent with the results observed following overexpression of the Y-All-F mutant, where all putative phosphotyrosine residues were mutated to phenylalanine (ephrinB2$_{(Y304,311,316,330,331F)}$) (Figure 17). When this mutant was overexpressed, HUVEC migration in response to monolayer wounding was also impaired. The full mutant, having both mutations at Y316 and Y330 rendering them un-phosphorylatable, showed a decrease in the rate of migration as compared to the wildype ephrinB2 overexpression thus supporting our previous observations following infection with the single mutated vectors. We also

wanted to know if the ephrinB2 mutant overexpressing cells migrate at all, or if the non-infected cells migrate around the overexpressing cells, thus resulting in an apparent delay in overall migration and wound healing. To address this, we performed an experiment where we seeded HUVEC on glass cover slips and repeated the wounding assay upon overexpression of ephrinB2 using adenoviral vectors. At the end of the assay, cells were fixed, permeabilized and stained for ephrinB2 using specific antibody. We found that although there is a delay in the migration of ephrinB2$_{(Y304,311,316,330,331F)}$ overexpressing cells, these cells indeed migrate and are found in the closed wound at the end of the assay (Figure 17B). Although the overall pattern of migration is consistent from one experiment to another, the times of closure differ by as much as 24 hours (Figure 16 and Figure 17). However, this could be due to the different passage number of the cells used in the experiment, which in the case of primary cells would be a factor, or the fact that the cell migration on plastic and glass may differ.

It is interesting to note that stimulation of endogenous ephrinB2 with EphB6-Fc receptors decreases cell migration while overexpression of wildtype ephrinB2 does not. This could be due to the fact that cells that were overexpressing ephrinB2 were not activated by its cognate Eph receptors and thus reverse signaling may not have occurred. It does remain possible however that some overexpressing cells could have been activated following binding by endogenous receptors on neighbouring cells. Although overexpression of the wildtype ephrinB2 in cells may not result in reverse signaling, it remains possible however, that the mutated forms, mainly ephrinB2$_{(Y316F)}$ and eprinB2$_{(Y330F)}$ acted in a dominant-negative fashion to sequester the signaling

molecules away from the endogenously expressed ephrinB2 ligand molecules and thus impaired their function in this manner. Alternatively, the effects of ephrinB2 may differ depending on the amounts of ephrinB2 being engaged, as it has been previously demonstrated that cells undergo different signaling responses depending on the degree of ephrin clustering. Receptor tyrosine phosphorylation has been proved to be stimulated by both dimeric and clustered multimeric ephrinB1, yet only ephrinB1 multimers (tetramers) promoted endothelial capillary-like assembly, cell attachment, and the recruitment of low-molecular-weight phosphotyrosine phosphatase (LMW-PTP) to receptor complexes (Stein *et al.*, 1998). Furthermore, co-clustering of ephrinB and Src occurs independently of rafts, but raft localization of ephrinB and SFK is required for proper regulation of ephrinB phosphorylation (Palmer *et al.*, 2002).

Figure 15. Activation of endogenous ephrinB2 results in inhibition of cell migration. HUVEC were grown to confluency on plates and the monolayers were scratch wounded with a pipette tip, washed, and stimulated with 0.01μg/ml, 0.1μg/ml, or 1.0μg/ml of EphB6-Fc, or the same concentrations of control IgG in the presence of 50ng/ml of VEGF. Wound closure was monitored every 24 hours and images were recorded using a Nikon camera fitted to a microscope at 40x magnification. The initial average wound size at time 0 was determined and used to subsequently calculate the percent closure over time for each sample (A). Panel (B) shows representative wound closure over time for VEGF only control. A p-value of <0.05 as compared to the equal doses of IgG stimulated cells is indicated by *. EphB6-Fc stimulation significantly slows down the migration of endothelial cells at 48 hours as compared to equal concentrations of IgG control.

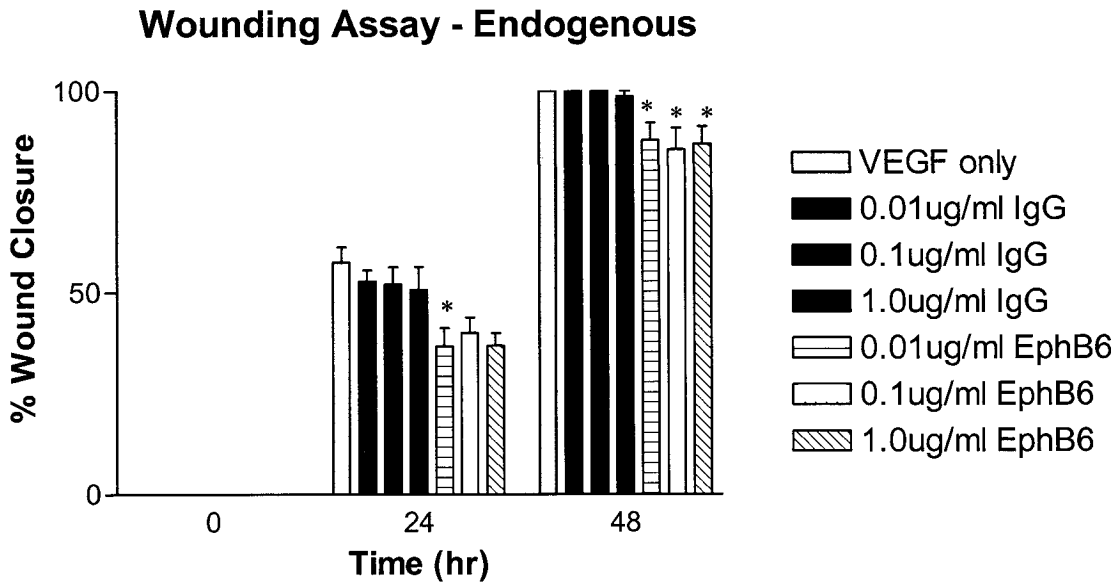
Wounding Assay - Endogenous
% Wound Closure
100
50
0
0
24
48
Time (hr)
*
*
*
VEGF only
0.01ug/ml IgG
0.1ug/ml IgG
1.0ug/ml IgG
0.01ug/ml EphB6
0.1ug/ml EphB6
1.0ug/ml EphB6

A

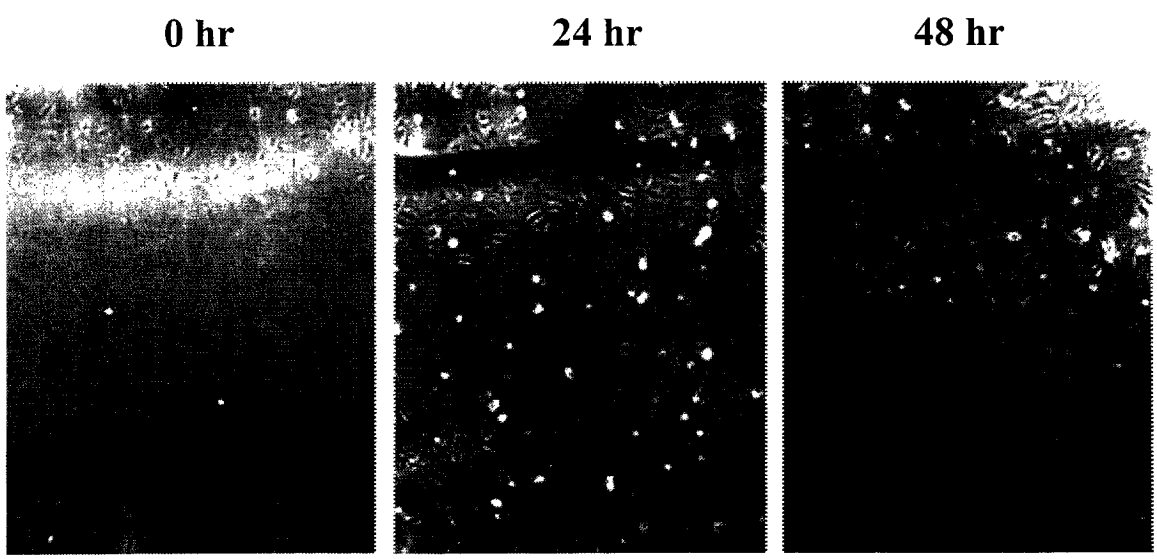
0 hr
24 hr
48 hr

B

Figure 16. Reverse signaling via ephrinB2 is required for HUVEC migration. HUVEC were grown to confluency on plates and either mock infected, infected with control adenoviral vector, or adenoviral vectors encoding ephrinB2 or its mutant forms. Cells were wounded with a pipette tip 24 hours post infection, washed, and cultured with maintenance media in the absence (A) or presence of 50ng/ml of VEGF (B). Wound closure was monitored every 24 hours and images were recorded using a Nikon camera fitted to a microscope at 40x magnification. The initial average wound size at time 0 was determined and used to subsequently calculate the percent closure over time for each sample. The * indicates a p-value <0.05, and ** indicates a p-value <0.001 as compared to the ephrinB2 wildtype infected cells. Overexpression of mutant ephrinB2 inhibited cell migration.

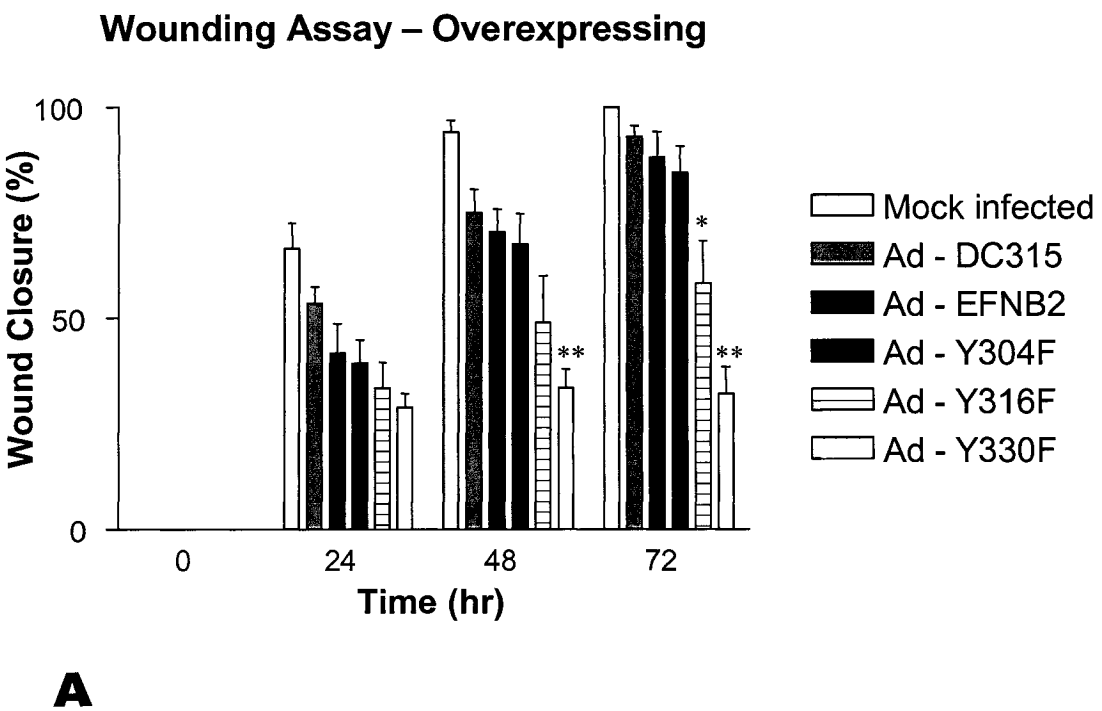
Wounding Assay – Overexpressing
100
50
0
Wound Closure (%)
0
24
48
72
Time (hr)
*
**
**
Mock infected
Ad - DC315
Ad - EFNB2
Ad - Y304F
Ad - Y316F
Ad - Y330F

A

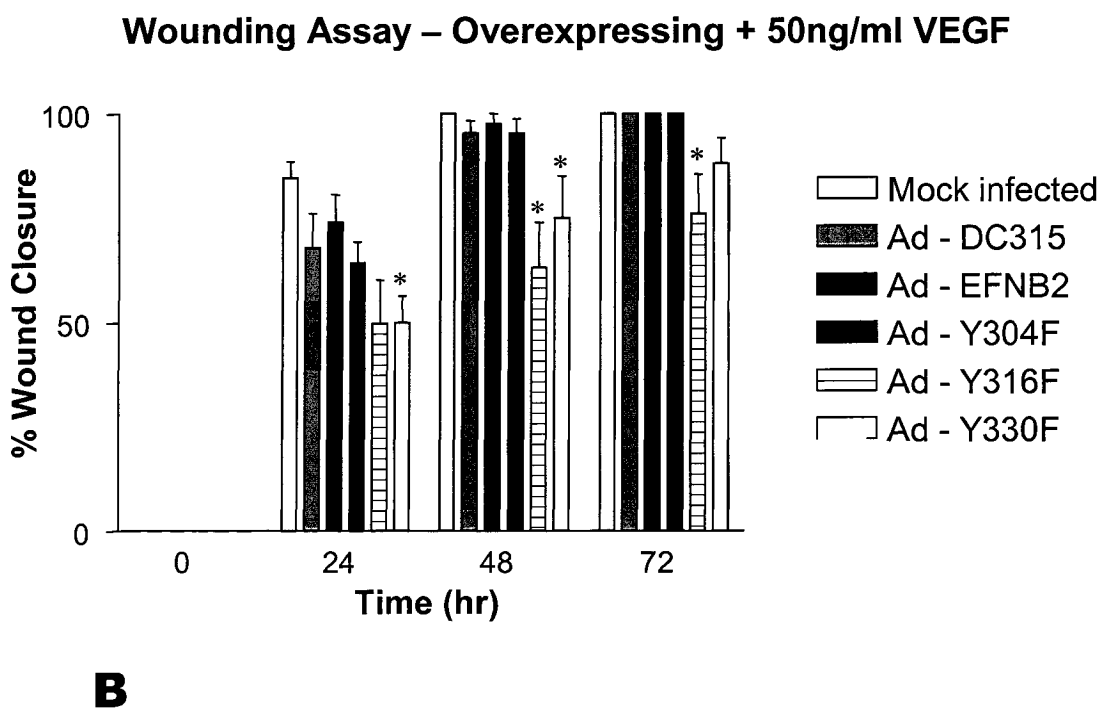
Wounding Assay – Overexpressing + 50ng/ml VEGF
100
50
0
% Wound Closure
0
24
48
72
Time (hr)
*
*
*
*
Mock infected
Ad - DC315
Ad - EFNB2
Ad - Y304F
Ad - Y316F
Ad - Y330F

B

Figure 17. Tyrosine phosphorylation of ephrinB2 is required for cell migration. HUVEC were grown to confluency on glass cover slips and infected with either control adenoviral vector, or adenoviral vectors encoding ephrinB2 or its full mutant ephrinB2$_{(Y304,311,316,330,331F)}$ (Y-All-F). Cells were wounded with a pipette tip 24 hours post infection, washed, and cultured with maintenance media in the presence of 50ng/ml of VEGF. Wound closure was monitored every 24 hours and images were recorded using a Nikon camera fitted to a microscope at 40x magnification. The initial average wound size at time 0 was determined and used to subsequently calculate the percent closure over time for each sample. The * indicates a p-value <0.05 as compared to the ephrinB2 wildtype or control infected cells (A). At the end of the experiment, cells were fixed, permeabilized, and stained with anti-ephrinB2 antibody (green), and Hoechst to visualize the nucleus (blue), and viewed with fluorescent microscope at 200x magnification to determine if the infected cells were found at the migrating edge of the wound (B). The arrow indicates wound direction. Migration in cells expressing the Y-All-F mutant was impaired as compared to wildtype ephrinB2 or control vector infected cells.

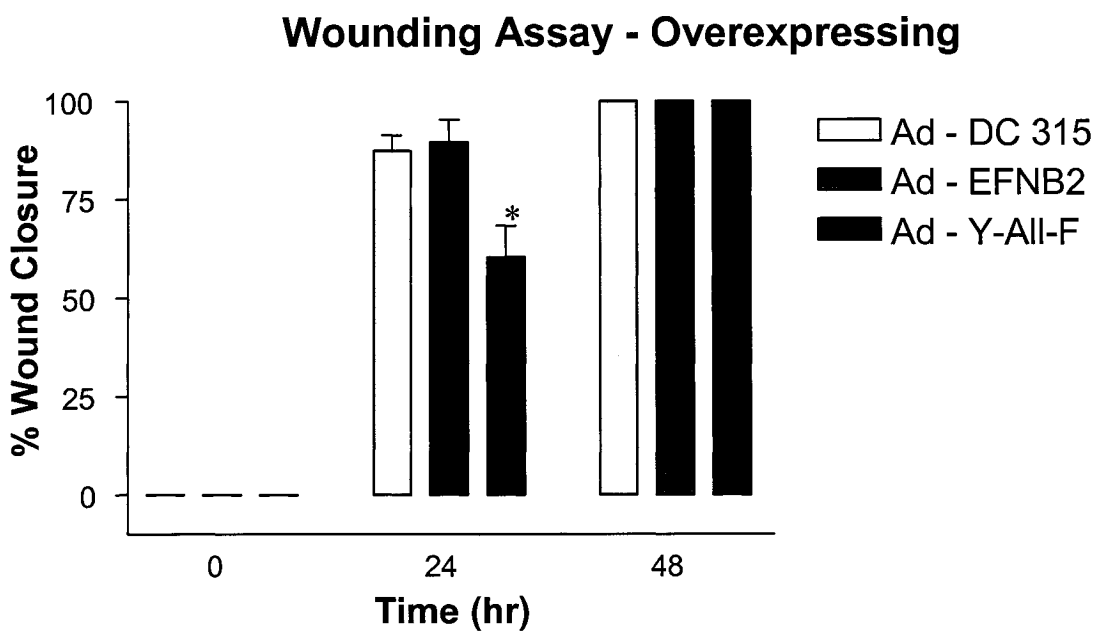
Wounding Assay - Overexpressing
% Wound Closure
100
75
50
25
0
0
24
48
Time (hr)
*
Ad - DC 315
Ad - EFNB2
Ad - Y-All-F

A

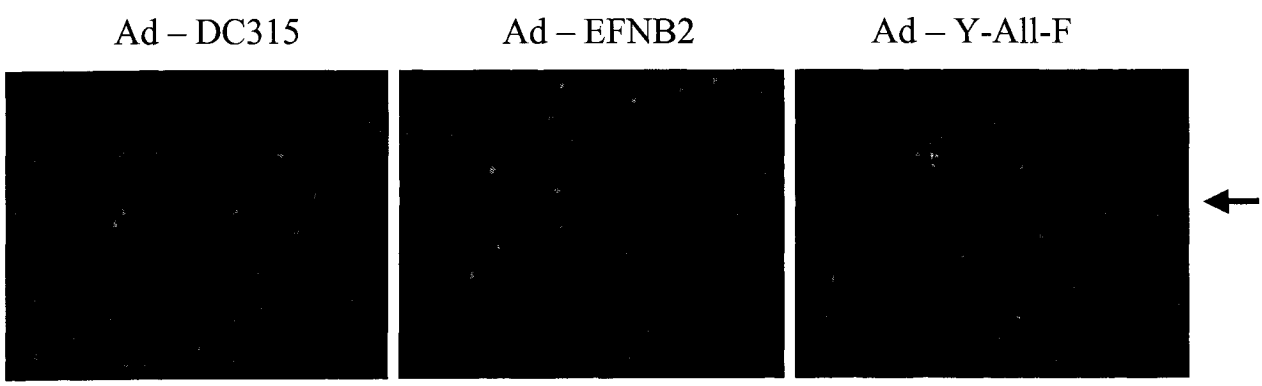
Ad – DC315
Ad – EFNB2
Ad – Y-All-F

B

5. Actin Cytoskeleton

As noted earlier, ephrinB2 overexpression following retroviral transduction and subsequent signaling altered the cytoskeletal phenotype in HDMEC thus suggesting a role in endothelial cell morphology and migration during angiogenesis. Therefore, we wanted to first confirm these findings using adenoviral expression vectors, and further use this tool to examine the molecules that may be playing a role in the observed cytoskeletal rearrangement. HDMEC were grown to confluence and infected with adenoviral vectors expressing ephrinB2 or its mutant versions, and 24 hours later, cells were fixed, permeabilized and stained for ephrinB2 expression, as well as actin cytoskeleton using phalloidin in order to determine if ephrinB2 colocalized with actin stress fibers. We were also able to quantify the percentage of cells that were infected with the adenoviral vectors following detection of ephrinB2 overexpression by immunofluorescent staining. We examined five fields of view in one slide of each adenoviral infected sample, and counted the FITC positive cells, and compared them to total number of cells in the field of view. It was found that Ad-EFNB2 overexpressing adenoviral vector infected 85±15% of the cells (%±SD), Ad-Y304F infected 95±3% of the endothelial cells, Ad-Y311F 90±8%, Ad-Y316F 93±7%, Ad-Y330F 81±16%, and Ad-Y331F infected 46±25% of the endothelial cells. It should also be noted that control Ad-DC315 infected cells showed some background fluorescence in 8±3% of the cells. With the exception of Ad-Y331F, all other adenoviral vectors had a high infection proportion (>80%). It should be noted that this adenoviral vector had the lowest expression of ephirnB2 in the western blot

analysis (Figure 9), so it is most likely that this low detection in cells is due to improper tittering of the virus instead of the protein being in a conformation that is not detected by immunofluorescence. As observed previously using retroviral vector transduction, overexpression of ephrinB2 using adenoviral vectors resulted in changes in the cell morphology (Figure 18). It was noted that cells that overexpressed ephrinB2 changed their morphology, and appeared to have decreased contact with neighbouring cells, with the exception of overexpression of ephrinB2$_{(Y331F)}$, which maintained cell-cell contact and appeared to have no major differences in cell morphology. However, this could be due to large percentage of cells being uninfected or not expressing a functional ephrinB2 protein following infection with this particular mutant ephrinB2 expressing virus. Despite the issues with this particular mutant, the majority of cells overexpressing ephrinB2 or its mutants following infection with the other viral constructs appeared somewhat smaller in size as compared to control cells, and their actin cytoskeleton seemed to have reduced numbers of stress fibers. This was apparent by the majority of the phalloidin staining appearing in a more diffuse pattern in the cytoplasm as compared to control infected cells (Figure 18C, top two panels). The bottom panel of Figure 18C shows that there is no "bleed-through" of the TRITC or FITC in the different channels of the microscope as there is clearly no overlap of red nor green in their respective channels. The expression of ephrinB2 following adenoviral vector infection showed two different patterns of expression, with very punctate staining in some cells (yellow arrow) and other cells showing more localized expression at membrane-edges (red arrow) (Figure 18 A, B). In both cases, diffuse cytoplasmic staining was also

apparent. In some cases it would appear that the ephrinB2 expression was colocalized with actin fibers (blue arrowhead), however this was not consistently observed in all infected cells (white arrowhead) (Figure 18 A, B).

In order to determine whether the ephrinB2 ligand was being expressed in and targeted to its proper cellular locale, we examined the expression of ephrinB2 in infected cells by immunofluorescence and acquisition of "Z-stacks" comprising 24 microscope images going through the cell, and later reconstructing the images into a 3D model using Imarus Software (Bitplane Inc., Zurich Switerzerland) (data not shown). We found that ephrinB2 can be found on the surface, however, there also appeared to be columnar pattern of staining going through the thickness of the endothelial cell that could not be explained. Importantly, the pattern of expression was not consistent with the expressed protein being localized to the trans golgi or endoplasmic reticulum, and does suggest that protein is being targeted to the cell surface and other as of yet unidentified cytoplasmic structures. As we initially concentrated on the expression of wild type ephrinB2, in the future it needs to be determined whether all the mutant versions of ephrinB2 similarly localize to the cell surface. This could be done by immunofluorescence, by using non-permeabilized cells, or detection by flow cytometry.

The apparent decreased formation of actin stress fibers led us to believe there was a possibility that changes in the ratio of F-actin/G-actin was occurring in infected cells upon overexpression of ephrinB2. In order to test this, we then infected HUVEC with adenoviral vectors expressing ephrinB2 wildtype, or its full mutant ephrinB2$_{(Y304,311,316,330,331F)}$ (Y-All-F) or control vector, and 24 hours later, cells were

collected and subsequently stained with flourescently-conjugated Phalloidin to label the F-actin or flourescently-conjugated DNase I to label the G-actin within the cells. Cells were then analyzed by flow cytometry to quantitate the amount of F- and G-actin respectively. Upon overexpression of ephrinB2 or its mutant form, there was no change in the F-actin/G-actin ratio as compared to control adenoviral infected cells (Figure 19). The histogram plots looked similar and when their mean peak values were compared, there was no significant difference between them. Although immunofluorescence suggested a decrease in F-actin, our failure to demonstrate this following FACS analysis could be due to the processing of the samples. In order to analyze the samples, trypsinization needed to be performed, and this is known to alter actin dynamics. Therefore, if the samples could be processed in a different way that does not alter the cell cytoskeleton, possibly by lifting the cells off the dishes by using cold EDTA, the immunofluorescence results could be confirmed. In addition, it is also possible that the effects on the F-actin/G-actin ratio are not detectable due to the presence of uninfected cells that are not overexpressing ephrinB2, and thus interfering with our detection. FACS analysis could be performed whereby we initially label the ephrinB2 positive cells with ephrinB2 specific antibody conjugated to one fluorfore, and then within this population of cells we could detect the F-actin and G-actin levels using phalloidin and DNAseI proteins conjugated to a different fluorofore that is easily distinguishable from the first. One could also perform western immunoblot analysis to determine if there is a change in the amount of F-actin and G-actin upon overexpression of ephrinB2 wildtype or its mutants.

Figure 18. EphrinB2 alters actin cytoskeleton. HDMEC were grown to confluency on cover slips and were either mock infected, infected at an MOI of 5 pfu/cell with control DC315 adenoviral vector, or adenoviral vectors encoding wildtype ephrinB2 or mutant ephrinB2 versions. Cells were fixed 24 hours later, permeabilized, and stained with anti-ephrinB2 antibody (green). Cells were also incubated with TRITC-conjugated Phalloidin to stain the cell F-actin cytoskeleton (red) and Hoechst to visualize the nucleus (blue) and viewed with fluorescent microscope at 400x magnification (A and B), and 1000x (C). Yellow arrows ( ) represent very punctate staining of ephrinB2 in some cells and red arrows (→) represent the more localized expression at membrane-edges that was observed. Blue arrowheads (▶) represent colocalized expression of ephrinB2 with actin fibers, and white arrowheads ( ) represent where this colocalization was not observed. The numbers below the pictures represent the mean percentage and standard deviation of infected ephrinB2 overexpressing (green) cells as compared to total number of cells in a given field of view (5 fields of view at 400x magnification). Overexpression of ephrinB2 led to modifications of cell shape and actin arrangement within the cells.

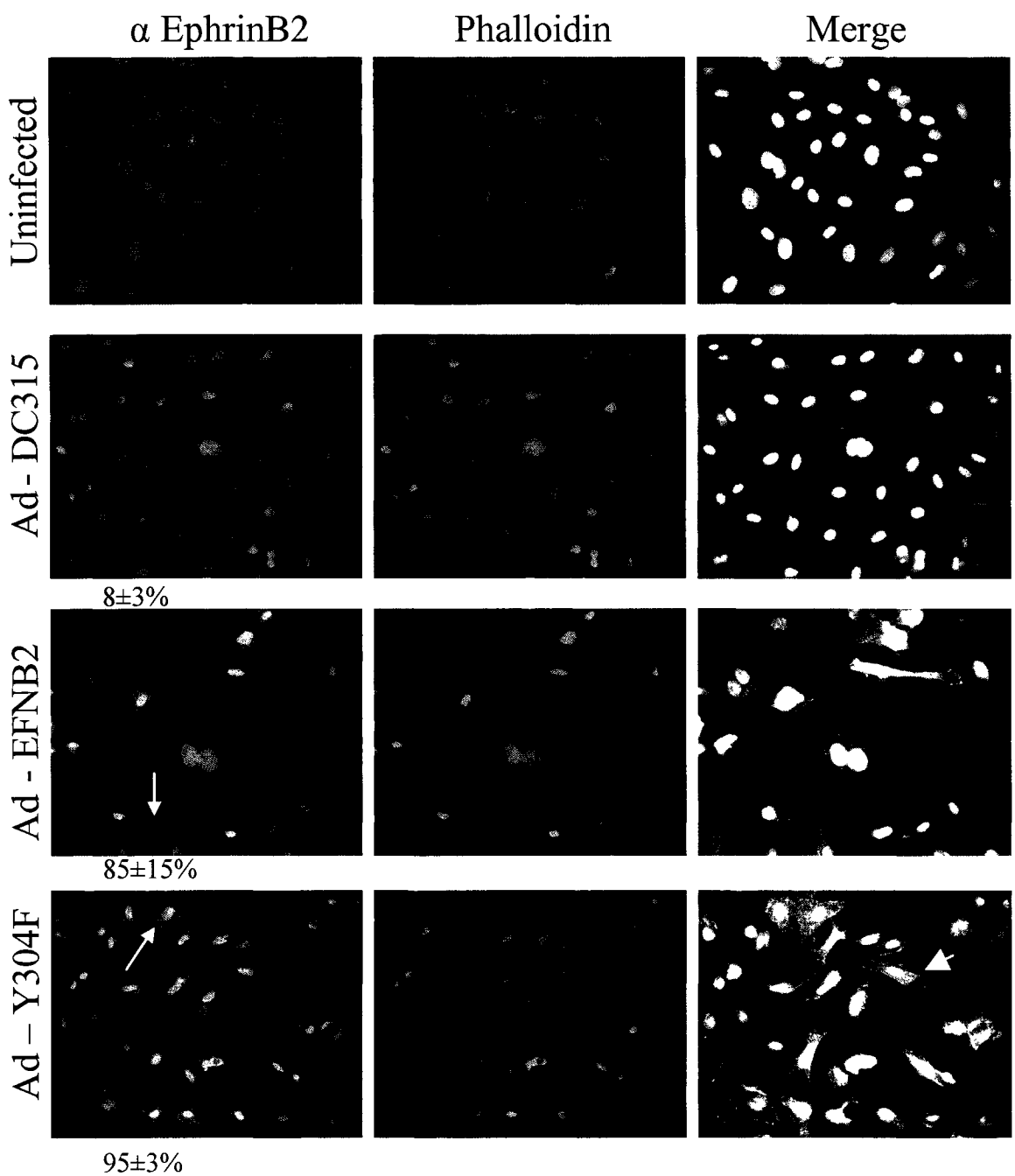
α EphrinB2
Phalloidin
Merge
Uninfected
Ad - DC315
8±3%
Ad - EFNB2
85±15%
Ad – Y304F
95±3%

A

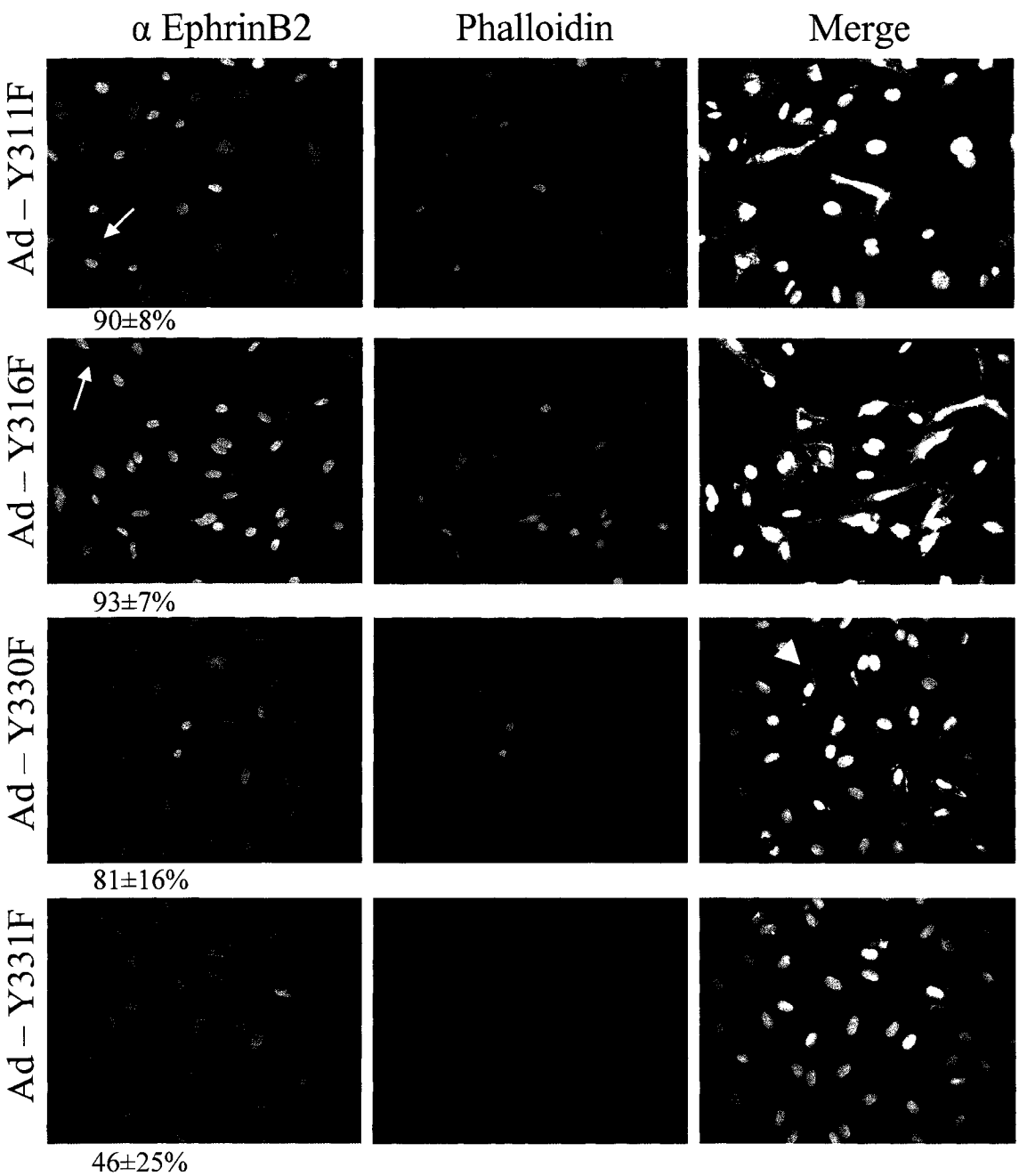
α EphrinB2
Phalloidin
Merge
Ad – Y311F
90±8%
Ad – Y316F
93±7%
Ad – Y330F
81±16%
Ad – Y331F
46±25%

B

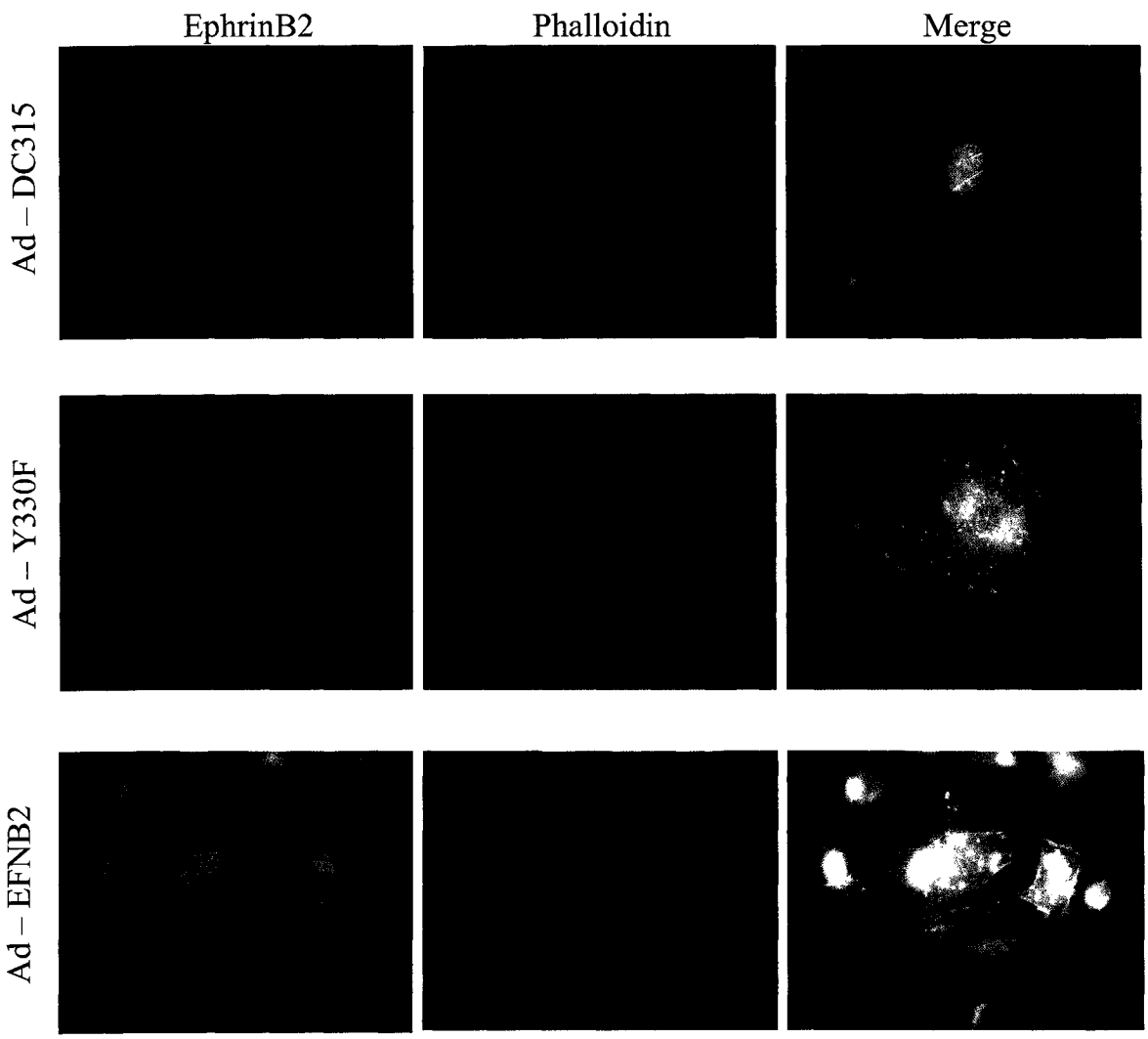

c

Figure 19. Overexpression of ephrinB2 does not alter the F-actin/G-actin ratio. HUVEC were grown to confluency and infected at an MOI of 5 pfu/cell with control adenoviral vectors or adenoviral vectors expressing wildtype ephrinB2 or its full mutant ephrinB2$_{(Y304,311,316,330,331F)}$ (Y-All-F). Cells were trypsinized 24 hours later, fixed, permeabilized and stained with either Alexa-488 conjugated Phalloidin to stain F-actin (A), or Alexa-488 conjugated DNase I to stain G-actin (B). Cells were then analyzed by flow cytometry on the FL1 channel. Overexpression of ephrinB2 does not affect the F-actin/G-actin ratio.

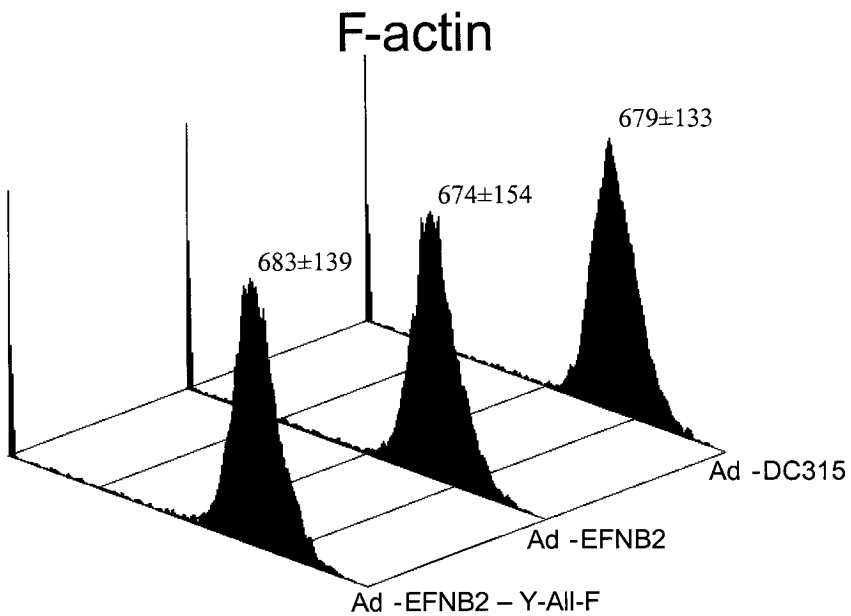
F-actin
679±133
674±154
683±139
Ad -DC315
Ad -EFNB2
Ad -EFNB2 – Y-All-F

A

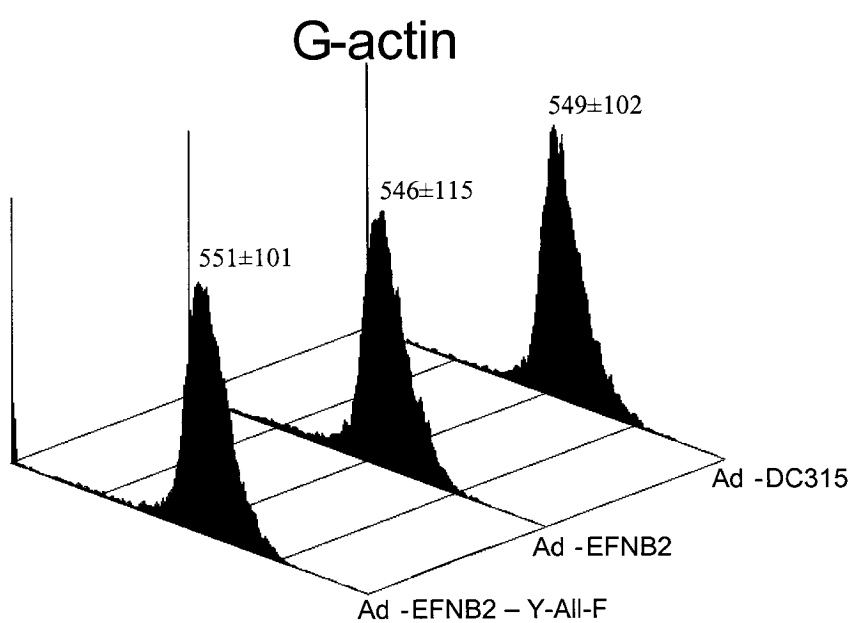
G-actin
549±102
546±115
551±101
Ad -DC315
Ad -EFNB2
Ad -EFNB2 – Y-All-F

B

6. Rho GTPases

The observed cytoskeletal changes following ephrinB2 overexpression led us to believe that there may be a role for the small molecule Rho GTPase family members in the reverse signaling mediated by ephrinB2. The three main members of this family are Rho, Rac, and Cdc42. We wanted to determine if any of these members play a role in ephrinB2 signaling, and especially in the physiological outcomes such as migration of endothelial cells. First we wanted to determine the effects of endogenous expression of ephrinB2 on the activity of small GTPases using an activity assay. HUVEC were grown to confluency and serum starved overnight. Cells were then incubated with increasing concentrations of EphB6-Fc chimeric protein to stimulate the ephrinB2 reverse signaling for 30 minutes. Cells were then lysed and active Rac was precipitated with GST-Pak fusion protein. Pak contains the Cdc42-Rac interacting binding domain (CRIB) of p21 activated kinase, and specifically binds GTP bound, that is active, Rac. Precipitates were separated by gel electrophoresis and active Rac was visualized following western blot analysis using a Rac specific antibody (data not shown). There was some evidence suggesting that increasing doses of EphB6-Fc decreased the amount of active, GTP bound Rac, however, the results were not conclusive. Future experiments to confirm this finding, and additional experiments using alternative doses of EphB6-Fc for stimulation and additional time points post-stimulation will help solidify this finding.

We also wanted to determine the role of the GTPase molecule Rho in endothelial cell migration. Similar to GST-Pak pull-down assay, GST-C21 pull-down

was attempted several times. C21 is a GTP binding domain of Rhothekin, a Rho target molecule that specifically binds active, GTP bound Rho. Even though the assay was attempted several times, it proved unsuccessful. As an alternative strategy, we investigated the localization of Rho during endothelial cell migration following activation of ephrinB2 reverse signaling using immunofluorescence with specific antibodies to Rho. It has been previously shown that during cell migration, active Rho localizes to the trailing edge of cells (Saito *et al.*, 2002; Riento and Ridley., 2003). To examine the expression of Rho, HDMEC were grown to confluency on cover slips and serum starved overnight. After wounding, cells were washed, and stimulated with 0.1μg/ml or 1.0μg/ml of EphB6-Fc, in the presence or absence of 50ng/ml of VEGF. Cells were fixed 30 minutes later, permeabilized and stained for Rho using a specific antibody and visualized with a fluorescent microscope. Cells that were along the wound edge were inspected (the location of scale bar in every panel indicates the site of the wound and the direction in which cells would be migrating). It was seen that increased concentrations of EphB6-Fc led to an increase in the levels of Rho being detected at the rear end of the cell, that is away from the wound edge, as shown by the arrows (Figure 20). Six images were taken along the wound edge for every condition and this increase in intensity of staining was seen in at least four images for every condition. This data is consistent with that describing Rho in the literature as the cells that are ready to migrate would recruit Rho to the lagging end of the migrating cells to reorganize actin cytoskeleton and cause blebbing and deadhesion (Lawrenson *et al.*, 2002). Taken together, our data could support a role for ephrinB2 reverse signaling in cell migration as usually when Rac activity

decreases, Rho activity increases, and as we previously noted the deactivation of Rac following stimulation of endogenously expressed ephrinB2, it would make sense that the Rho activation is increased upon stimulation of reverse signaling through ephrinB2.

Figure 20. Stimulation of endogenous ephrinB2 reverse signaling leads to Rho relocalization. HDMEC were grown to confluence on cover slips and serum starved overnight. Cells were wounded with a pipette tip, washed, and stimulated with 0.1μg/ml or 1.0μg/ml of EphB6-Fc, in the presence or absence of 50ng/ml of VEGF. Cells were fixed 30 minutes later, permeabilized and stained with anti-Rho antibody. Fluorescently-tagged secondary antibody was used for visualization on an inverted fluorescent microscope at 1000x magnification. Cells that were along the wound edge were inspected (the location of scale bar in every panel indicates the wound side) and black arrowheads (▼) indicate wound direction. Increased dose of EphB6-Fc, especially in VEGF stimulated cells, leads to more Rho being detected at the trailing rear end of the cell, that is, away from the wound edge, shown by the yellow arrows ( ).

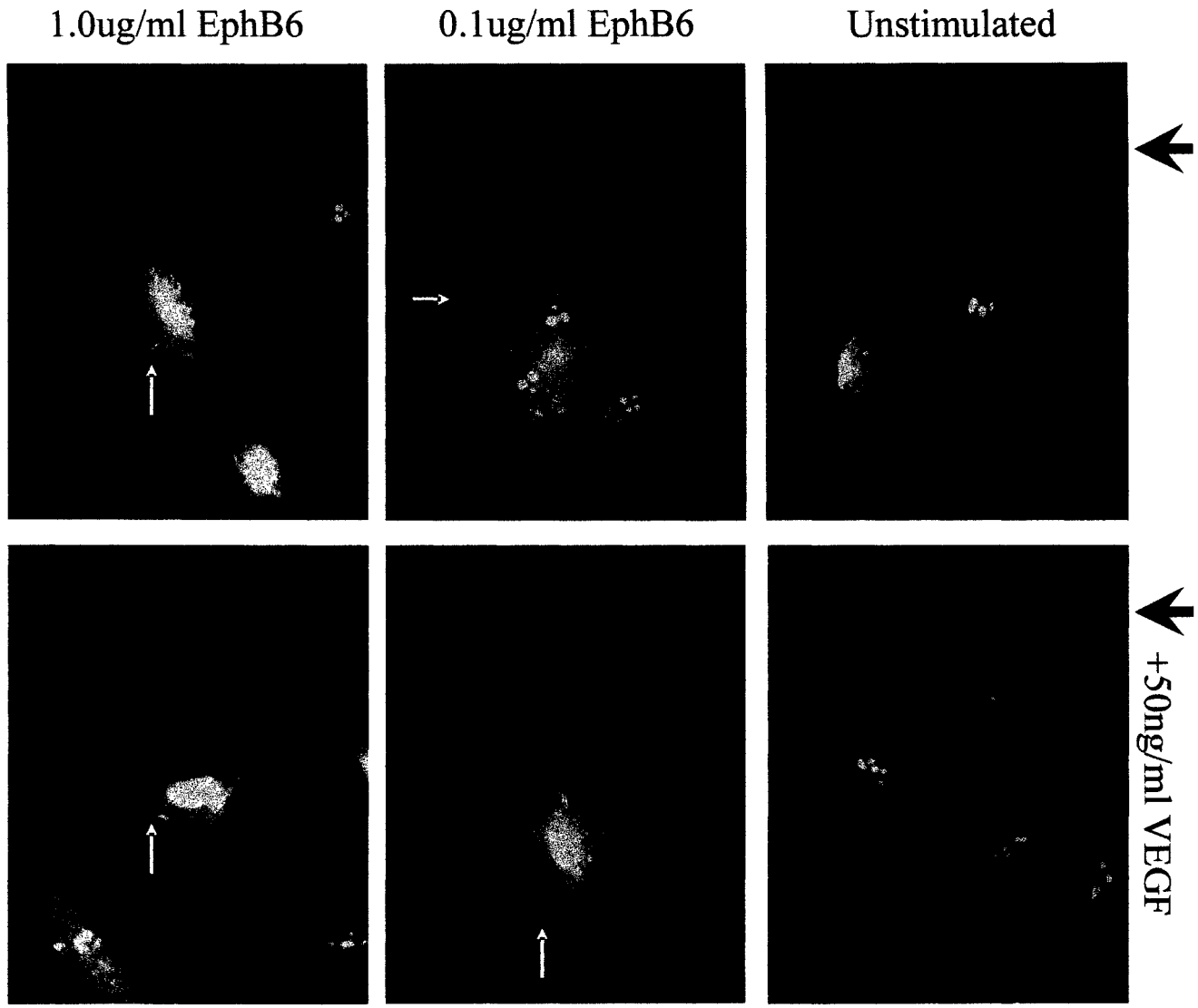
1.0ug/ml EphB6
0.1ug/ml EphB6
Unstimulated
+50ng/ml VEGF

Discussion

The cellular responses to Eph/ephrin signaling are important in mediating a wide range of biological activities, including angiogenesis, cell segregation, and cell attachment, shape and motility. Furthermore, elevated Eph/ephrin expression is associated with angiogenesis and tumour vasculature in many types of human cancers (Surawska *et al.*, 2004). Therefore, it is not surprising given the importance of angiogenesis in solid tumor growth that we observed the upregulation of ephrinB2 in endothelial cells following stimulation with the potent angiogenic factor VEGF (Figures 3-5). It is possible that the growing tumour would release VEGF, which would stimulate upregulation of ephrinB2 in adjacent endothelium, so that ephrinB2 could mediate the signaling resulting in motility of endothelial cells and subsequent angiogenesis to form neovessels within the tumor.

Our group has extensively studied the role of ephrinB2 reverse signaling in endothelial cell proliferation, survival and migration. Work by others in the laboratory has shown that ephrinB2 reverse signaling did not play a role in endothelial cell proliferation or survival (C. Addison and C. Delaney, personal communication). Extensive studies aimed at dissecting the roles of ephrinB2 in proliferation or survival of endothelial cells through activation of reverse signaling using Eph-Fc receptors revealed that there were no significant differences between unstimulated, control IgG stimulated or Eph-Fc stimulated cells (unpublished data). This led us to hypothesize that upregulation of ephrinB2 following stimulation of

endothelial cells with the potent angiogenic factor VEGF may have a role in endothelial cell migration during angiogenesis.

It has been proposed that the increased ratio of receptors to ligands during Eph overexpression may result in tumour sensitivity to ligand-induced stimulation and a consequently higher degree of tissue invasiveness, with decreased attachment and increased motility (Surawska *et al.*, 2004). This effect is likely due to the forward signaling through the receptor. However, it is unclear how changing the ratio of receptor to ligand affects the reverse signaling cascade. It is reasonable to hypothesize that upon overexpression of the ephrinB2 ligand, and subsequent change in the ratio of receptors to ligands, cells would have increased attachment to the substratum and decreased cell motility. However, this was not observed in our case. When ephrinB2 was overexpressed using adenoviral vectors, endothelial cells decreased their attachment to the extracellular matrix. Furthermore, endothelial cell migration was only affected upon overexpression of mutant eprhinB2$_{(Y316F)}$, ephrinB2$_{(Y330F)}$, and ephrinB2$_{(Y304,311,316,330,331F)}$ molecules (Figures 16 and 17), or when endogenous ephrinB2 was stimulated with soluble EphB6-Fc receptors. The fact that inhibition of migration was only observed following activation of reverse signaling by stimulation with EphB6-Fc or overexpression of signaling impaired mutants, suggests that simple overexpression of wild-type ephrinB2 by adenoviral infection may not be sufficient to induce reverse signaling and affect cell migration. However, this also implies that overexpression of the ephrinB2 tyrosine mutants may act in a dominant-negative fashion to impair the ability of the endogenous ephrinB2 to function in an appropriate manner. It is possible that they prevent forward

signaling of the receptor because they cannot cluster properly. It is also possible that mutations in ephrinB2 cause steric hindrances to the molecule rendering it unusable in cell communication, either forward or reverse. It remains to be determined what the effect on reverse signaling is when soluble EphB receptors are added to the cells that are expressing mutant versions of ephrinB2. Taken together, our data suggest that reverse signaling is needed to mediate the physiological outcome such as migration of endothelial cells, and that overexpression of ephrinB2 alone is insufficient to effect migration of endothelial cells. It is also possible that these signaling events are cell-type specific and one signaling cascade is mediated in tumour cells, whereas another exists in endothelial cells.

As previously mentioned in the introduction, blood vessel formation and sprouting requires the phosphorylation of the cytoplasmic domain of ephrinB ligands by the Src family kinases, implicating a role for ephrinB reverse signaling in angiogenesis (Palmer *et al.*, 2002). Furthermore, it has been shown that the cytoplasmic domain of ephrinB2 is required for angiogenic remodeling *in vivo* (Adams *et al.*, 2001), suggesting that ephrinB2 reverse signaling is crucial for endothelial cell communication and vessel formation. EphrinB proteins (B1-B3) have well-conserved cytoplasmic domains that include 33 amino acids at the C-terminus showing a 95% identity among the ephrinB proteins (Beckmann *et al.*, 1994). In ephrinB1, tyrosine residues at positions 312, 317, and 331 are phosphorylated after engagement with the Eph receptor ectodomain *in vivo*, and Y331 in the PDZ-binding motif has been determined to be the major *in vivo* phosphorylation site of ephrinB1 bound to the EphB2 receptor, and is proposed to be

involved in multimerization of the ephrinB molecule (Kalo *et al.*, 2001). Phosphorylation of the second tyrosine in the YYKV motif, Y332 could not be detected. These tyrosines correspond to positions 311, 316, 330, and 331 of ephrinB2, and it can therefore be postulated that these residues become phosphorylated upon activation of reverse signaling of ephrinB2 in a similar manner. Undetectable phosphorylation at Y332 of ephrinB1 supports our finding that overexpression of ephrinB2$_{(Y331)}$ had little effect, and did not alter cell shape or cell contact (Figures 8, 18B). It should be noted that this adenovirus expressing this mutant had the lowest infection rate, this was likely due to improper titration of the virus. However, the cells that were observed, showed little phenotypic changes associated with other mutants or the wildtype. This suggests that phosphorylation at this particular tyrosine residue of ephrinB2, found at the extreme C-terminus PDZ binding domain (YY$_{331}$KV), is not important in signaling to downstream effectors, and changing this residue to phenylalanine does not significantly disrupt the subsequent binding of PDZ containing proteins. However, Y330 of ephrinB2 could be involved in both phosphorylation-dependent and phosphorylation independent signaling. Mutation of this tyrosine residue to phenylalanine led to a decrease in endothelial cell migration (Figure 16). This could be due to lack of multimerization of ephrinB2 molecules, a phosphorylation-dependent event, or due to the disruption of the Y$_{330}$YKV PDZ binding domain, a phosphorylation-independent event. By disrupting the PDZ binding domain, it is possible that the PDZ-RGS3 protein signaling is inactivated. PDZ-RGS3 is a protein that regulates trimeric G proteins during cell migration (Lu *et al.*, 2004), a role that is supported by our data where

disruption of interactions via the PDZ domain by mutation led to the inhibition of cell migration.

Previous work has demonstrated that phosphorylated Y304 and Y316 ephrinB2 peptides bound to the SH2 domain of the adaptor protein Grb4 in a similar manner (Song, 2003) and additional phosphorylation at Y311 did not enhance this binding. Grb4 is involved in transducing reverse signals into ephrinB expressing cells and this interaction may have functional significance by regulating the cytoskeleton during cell adhesion and cell migration (Cowan and Henkemeyer, 2001). Although when presented as a peptide, phosphorylated Y304 has been found to bind Grb4 directly (Su *et al.*, 2004), it is possible that phosphorylated Y316 of the full length ephrinB2 may be primarily responsible for binding Grb4, since the overexpression of mutated Y304 of ephrinB2 had no effect on cell migration. It is possible that this particular tyrosine residue is not available for phosphorylation when present in the conformational context of the full-length protein. Our data would suggest that the possible binding of Grb4 to phosphorylated Y316 transduces a physiologically relevant signal that leads to migration as this process was impaired following overexpression of the ephrinB2$_{(Y316F)}$ mutant. However, it is also possible that another unknown adaptor molecule binds to the phosphorylated Y316 and transduces the signal leading to migration of endothelial cells. Unphosphorylated ephrinB2 adopts a well-packed β-hairpin structure (Song *et al.*, 2002) but this structure is radically disrupted upon tyrosine phosphorylation, regardless of the exact position of the phosphorylated site (Song, 2003). It is therefore also possible that the phosphorylation of Y316 leads to "opening up" of ephrinB2 molecule, resulting in the

exposure of other tyrosine residues, and their subsequent phosphorylation which facilitates binding of other proteins and then activates the reverse signaling cascade.

The Rho family of small GTPases has a central role in control of the dynamic reorganization of the actin cytoskeleton required for cell migration and adhesion (Hall and Nobes, 2000). The activation and direct binding of guanine nucleotide exchange factors (GEFs) is one of the major mechanisms by which Eph receptors and ephrins regulate migration (Noren and Pasquale, 2004) and may underlie a key aspect of Eph-ephrin function: the localized regulation of the actin cytoskeleton at the sites of cell-cell contact. A possible connection to Rac is through the SH2/SH3 adaptor Grb4, which associates with ephrinB tyrosine phosphorylated motifs (Song, 2003). Grb4 (also known as Nck-2), which is closely related to Nck, may recruit a Rac exchange factor such as αPix to the ephrinB. Rac activity stimulated by ephrins may be responsible for transcytosis of activated EphB-ephrinB receptor complexes into ephrinB expressing cells (Marston *et al.*, 2003; Zimmer *et al.*, 2003). In most cases, Eph-ephrin signaling concurrently affects Rho, Rac, and Cdc42 and can shift balance between their activated states. Furthermore, in nonneuronal cells, increased Rac1 activation downstream of Eph receptors promotes cell spreading and migration (Brantley-Sieders *et al.*, 2004) and inhibition of Rac1 decreases cell spreading and migration (Deroanne *et al.*, 2003). This could be supported with our data where activation of reverse signaling via endogenous ephrinB2, although inconclusive, suggested a decrease in Rac activity as well as slow down the migration of endothelial cells (Figure 15). It remains to be seen whether this decrease in Rac activation can be confirmed in the endogenous expression of ephrinB2 and further

whether the overexpression of ephrinB2 or its mutants via adenoviral vector infection has the same outcome on Rac activity. Our future work will determine to what degree tyrosine phosphorylation is responsible for this deactivation of Rac activity and using the various point mutants we will be able to determine the residues in ephrinB2 required for mediating this activity.

Recently, it was proposed that by phosphorylation/dephosphorylation of the ephrinB cytoplasmic domain, the reverse signaling could be controlled and switched between two critical pathways, one PDZ-dependent pathway leading to G-protein coupled receptor signaling and another phosphorylation-dependent pathway that modulates cytoskeletal dynamics (Palmer *et al.*, 2002). Stimulation of ephrinB1 reverse signaling resulted in a marked loss of polymerized actin as revealed by the disassembly of stress fibers, which normally span the length of the cell (Cowan and Henkemeyer, 2001). Furthermore, prolonged exposure to EphB2-Fc resulted in rounding up, shrinking and loss of adhesive contact in ephrinB1 expressing cells, while non-expressing cells were unaffected. We observed similar effects on actin cytoskeleton upon overexpression of ephrinB2 or its tyrosine mutant versions. We found that cells seem to change their actin cytoskeleton (Figures 8 and 18), and disassemble their stress fibers (Figure 18C), thus supporting a role for ephrinB reverse signaling in cytoskeletal remodeling and cell migration.

In addition to the PDZ proteins, another important regulator of cell adhesion and movement has been discovered to interact with ephrinB1 in a phosphorylation-independent manner. The *Xenopus* dishevelled protein has been recently shown to form a complex with the ephrinB ligand and to mediate cell repulsion via activating

RhoA (Tanaka *et al.*, 2003). Although we tried to detect Rho activation using GST pull-down assay, we were unable to successfully perform the experiment. However, using immunocytochemistry, we observed that Rho expression was more localized at the back or trailing edge of migrating endothelial cells upon stimulation with soluble EphB6-Fc receptors (Figure 20). Thus our data would support the notion that ephrinB reverse signaling can modulate the activity of the Rho family of proteins.

Taken together, our results led us to propose a role for ephrinB2 reverse signaling in endothelial cells. Upon stimulation by EphB6 receptor or its soluble EphB6-Fc substitute, the cytoplasmic tail of ephrinB2 undergoes phosphorylation on its tyrosine residues, most likely Y304, or the newly proposed Y316 and Y330, by Src. SH2 containing adaptor proteins, such as Grb4, bind to the phosphotyrosine site and recruit other proteins, such as Pak1 or αPix, which lead to subsequent downstream deactivation of Rac and activation of Rho. This in turn leads to slowing down of migration of endothelial cells (Figure 21). It should be noted that some of this is highly speculative, and was not directly assayed in these experiments.

There is also a possibility that some of these effects are secondary to blockade of ephrin-mediated forward signaling. For example, the soluble EphB6 receptor could also be blocking ephrinB2 binding to Eph receptors on adjacent cells in the culture, thus preventing forward signaling by receptors. As a result, the observed effects on cell migration following EphB6-Fc stimulation may be a result of inhibition of forward signaling instead of reverse signaling via ephrinB2. The effects on cell migration and shape that are induced in cells that overexpress wildtype and mutant forms of ephrinB2 following adenoviral infection, could be secondary to a

failure of forward signaling due to interference with trafficking of the endogenous ephrinB2 protein to the cell surface or a general interference with normal cellular function. To address this, it needs to be demonstrated that processing through the secretory pathway is normal for these transgenes, that is, to find out if they are found on the cell surface, and are capable of inducing normal forward signaling through EphB receptors on adjacent cells. As previously mentioned in the results section, confirmation of surface expression of ephrinB2 could be accomplished by immunofluorescence in the absence of cell permeabilization. Using our 3D images of ephrinB2 expression (data not shown), we have some idea that ephrinB2 is expressed at the surface of the cells. This should in fact enhance forward signaling, and if the results that are seen are due to this, then all the infected cells should have the same phenotype as all should induce forward signaling the same way, unless there was some conformational issue such as an inability to cluster. Another way to address the issue of blocking or enhancing the forward signaling pathway is to use a non-human, non-endothelial cell line that does not express any of the Eph receptors or Eph ligands. By introducing the transgenic human ephrinB2 and stimulating with soluble human EphB receptors, we can be certain that the results are due to reverse signaling alone. One candidate cell line could be Chinese hamster ovary (CHO) cell line that has been shown to have no expression of endogenous EphB receptors (Sturz *et al.*, 2004). One limitation with this system is that the responses observed in this cell line may differ from the human endothelial physiological response.

In our current studies, we have used an experimental approach that has been used extensively by other laboratories, that was designed to create a situation

whereby reverse signaling predominates in the cultures, however, as mentioned, we were unable to asses this directly using approaches to identify phosphorylation of ephrinB2. Multiple attempts were made by other lab members to examine tyrosine phosphorylation of the endogenous or adenoviral vector expressed ephrinB2 protein in endothelial cells. Endothelial cells were stimulated with soluble EphB6-Fc receptors, cells were lysed and ephrinB2 was immunoprecipitaed using ephrinB2 specific antibody, and blots were subsequently probed for tyrosine phosphorylation with PY-20 specific antibody which recognizes phosphorylated tyrosine residues. These results however, proved inconclusive. Recently, another approach was also attempted whereby ephrinB2 was immunoprecipitated in a similar fashion, but blots were probed using a phospho-specific ephrinB antibody. Preliminary results suggested that some ephrinB2 phosphorylation occurred as early as 10 minutes post EphB6-Fc stimulation, however, these results await confirmation and more complete characterization using additional doses of EphB6-Fc receptor and examination at alternative time points (Zhao and Addison, personal communication). Nevertheless, this important issue needs to be resolved in the future in order to ascertain if the effects on endothelial cell migration are a result of forward or reverse signaling induced by ephrinB/EphB interactions.

Our data suggests that angiogenic factors may modulate the expression of cell-cell communication molecules, specifically ephrinB2 and that reverse signaling induced via ephrinB2 following binding of its cognate receptor leads to biological changes in endothelial cells that may alter their attachment, their morphology and their migration through activation of cytoskeletal associated transduction molecules.

These changes may contribute to increase angiogenesis. It is possible that VEGF, which induces angiogenesis, upregulates ephrinB2 to signal to the migrating endothelial cells to stop migration after they come in contact with other receptor expressing cells, either tumour or endothelial, and subsequently organize to form vessels. In the absence of the stop signal, endothelial cells might keep migrating and never organize into functional vessels. However, this phenomenon needs to be further characterized and the mechanism of reverse signaling by ephrinB2 in endothelial cells requires further dissection. Despite the progress made in understanding the Eph/ephrin function in their role in cancer, due to their complex nature, much remains to be understood about the mechanisms and signaling processes. Our results will hopefully contribute to the understanding of the importance of the interaction of ephrinB ligands and EphB receptors, and will hopefully identify novel targets for future therapeutic interventions.

Figure 21. Potential mechanism of ephrinB2 reverse signaling. Upon stimulation by EphB6 receptor or its soluble EphB6-Fc substitute, the cytoplasmic tail of ephrinB2 undergoes phosphorylation on its tyrosine residues, most likely by Src. SH2 containing adaptor proteins, such as Grb4, bind to the phosphotyrosine site which leads to subsequent downstream deactivation of Rac, and activation of Rho leading to a decrease in the rate of migration of endothelial cells.

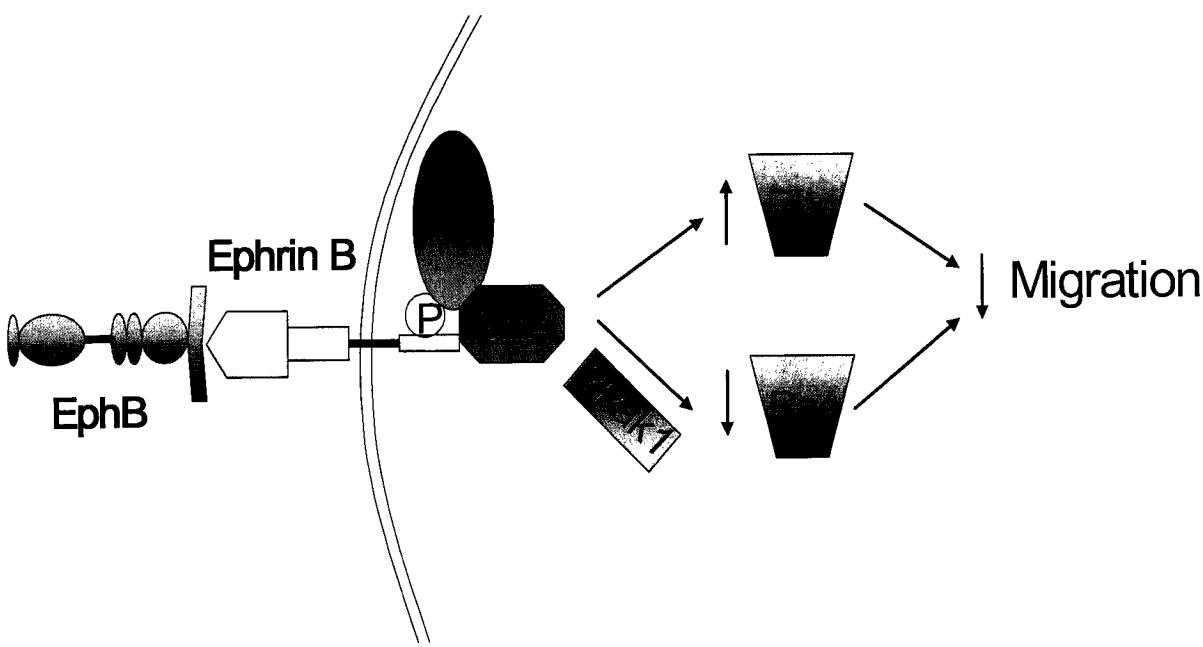
Ephrin B
EphB
P
Migration

References

1. Adams, R.H., Diella, F., Hennig, S., Helmbacher, F., Deutsch, U., Klein, R. (2001) The cytoplasmic domain of the ligand ephrinB2 is required for vascular morphogenesis but not cranial neural crest migration. *Cell.* **104**, 57-69
2. Adams, R.H., Wilkinson, G.A., Weiss, C., Diella, F., Gale, N.W., Deutsch, U., Risau, W., Klein, R. (1999) Roles of ephrinB ligands and EphB receptors in cardiovascular development: demarcation of arterial/venous domains, vascular morphogenesis, and sprouting angiogenesis. *Genes and Development.* **13**, 295-306
3. Arthur, W.T., Petch, L.A., Burridge. K. (2000) Integrin engagement suppresses RhoA activity via a c-Src-dependent mechanism. *Curr Biol.* **10,** 719-722
4. Batlle, E., Henderson, J.T., Beghtel, H., van den Born, M.M., Sancho, E., Huls, G., Meeldijk, J., Robertson, J., van de Wetering, M., Pawson, T., Clevers, H. (2002) Beta-catenin and TCF mediate cell positioning in the intestinal epithelium by controlling the expression of EphB/ephrinB. *Cell.* **111,** 251-263
5. Beckmann, M.P., Cerretti, D.P., Baum, P., Vanden Bos, T., James, L., Farrah, T., Kozlosky, C., Hollingsworth, T., Shilling, H., Maraskovsky, E., *et al.* (1994) Molecular characterization of a family of ligands for eph-related tyrosine kinase receptors. *EMBO J.* **13**, 3757-3762
6. Bong, Y.S., Park, Y.H., Lee, H.S., Mood, K., Ishimura, A., Daar, I.O. (2004) Tyr-298 in ephrinB1 is critical for an interaction with the Grb4 adaptor protein. *Biochem J.* **377**, 499-507
7. Brantley-Sieders, D.M., Caughron, J., Hicks, D., Pozzi, A., Ruiz, J.C., Chen, J. (2004) EphA2 receptor tyrosine kinase regulates endothelial cell migration and vascular assembly through phosphoinositide 3-kinase-mediated Rac1 GTPase activation. *J Cell Sci.* **117,** 2037-2049
8. Cho, K.O., Hunt, C.A., Kennedy, M.B. (1992) The rat brain postsynaptic density fraction contains a homolog of the Drosophila discs-large tumor suppressor protein. *Neuron.* **9**, 929-942
9. Cory, G.O., Garg, R., Cramer, R., Ridley, A.J. (2002) Phosphorylation of tyrosine 291 enhances the ability of WASp to stimulate actin polymerization and filopodium formation. Wiskott-Aldrich Syndrome protein. *J Biol Chem.* **277**, 45115-45121
10. Cowan, C.A., Henkemeyer, M. (2001) The SH2/SH3 adaptor Grb4 transduces B-ephrin reverse signals. *Nature.* **413,** 174-179
11. Davis, S., Gale, N.W., Aldrich, T.H., Maisonpierre, P.C., Lhotak, V., Pawson, T., Goldfarb, M., Yancopoulos, G.D. (1994) Ligands for EPH-related receptor tyrosine kinases that require membrane attachment or clustering for activity. *Science* **266**, 816-819
12. De Vries, L., Gist Farquhar, M. (1999) RGS proteins: more than just GAPs for heterotrimeric G proteins. *Trends Cell Biol.* **9**, 138-144

13. Deroanne, C., Vouret-Craviari, V., Wang, B., Pouyssegur, J. (2003) EphrinA1 inactivates integrin-mediated vascular smooth muscle cell spreading via the Rac/PAK pathway. *J Cell Sci.* **116**, 1367-1376
14. Dev, K.K. (2004) Making protein interactions druggable: targeting PDZ domains. *Nat Rev Drug Discov.* **3**, 1047-1056
15. Folkman, J. (1971) Tumour angiogenesis: therapeutic implications. *New Engl. J. Med.* **285**, 1182-1186
16. Folkman, J. (1990) What is the evidence that tumors are angiogenesis dependent? *J. Natl. Cancer Inst.* **82**, 4-6
17. Folkman, J. (1995) Angiogenesis in cancer. *Nat. Medicine.* **1**, 27-31
18. Folkman, J., D'Amore, P.A., (1996) Blood vessel formation: what is its molecular basis? *Cell.* **87**, 1153-1155
19. Fuller, T., Korff, T., Kilian, A., Dandekar, G., Augustin, H.G. (2003) Forward EphB4 signaling in endothelial cells controls cellular repulsion and segregation from ephrinB2 positive cells. *J Cell Sci.* **116**, 2461-2470
20. Gimbrone, M.A., Jr., Leapman, S.B., Cotran, R.S. and Folkman, J. (1972) Tumor dormancy in vivo by prevention of neovascularization. *J. Exp. Med.* **136**, 261-276
21. Hall, A., Nobes, C.D. (2000) Rho GTPases: molecular switches that control the organization and dynamics of the actin cytoskeleton. *Philos Trans R Soc Lond B Biol Sci.* **355**, 965-970
22. Hanahan, D., Folkman, J. (1996) Patterns and emerging mechanisms of the angiogenic switch during tumourigenesis. *Cell.* **86**, 353-364
23. Himanen, J.P., Nikolov, D.B. (2003) Eph receptors and ephrins. *Int J Biochem Cell Biol.* **35,** 130-134
24. Holland, S.J., Gale, N.W., Mbamalu, G., Yancopoulos, G.D., Henkemeyer, M., Pawson, T. (1996) Bidirectional signaling through the Eph family receptor Nuk and its transmembrane ligands. *Nature.* **383**, 722-725
25. Irie, F., Yamaguchi, Y. (2002) EphB receptors regulate dendritic spine development via intersectin, Cdc42 and N-WASP. *Nat Neurosci.* **5**, 1117-1118
26. Itoh, M., Nagafuchi, A., Yonemura, S., Kitani-Yasuda, T., Tsukita, S., Tsukita, S. (1993) The 220-kD protein colocalizing with cadherins in non-epithelial cells is identical to ZO-1, a tight junction-associated protein in epithelial cells: cDNA cloning and immunoelectron microscopy. *J Cell Biol.* **121**, 491-502
27. Kalo, M.S., Yu, H.H., Pasquale, E.B. (2001) In vivo tyrosine phosphorylation sites of activated ephrinB1 and EphB2 from neural tissue. *J. Biol. Chem.* **276**, 38940-38948
28. Lawrenson, I.D., Wimmer-Kleikamp, S.H., Lock, P., Schoenwaelder, S.M., Down, M., Boyd, A.W., Alewood, P.F., Lackmann, M. (2002) Ephrin-A5 induces rounding, blebbing and de-adhesion of EphA3-expressing 293T and melanoma cells by CrkII and Rho-mediated signalling. *J Cell Sci.* **115**, 1059-1072
29. Lin, D., Gish, G.D., Songyang, Z. and Pawson, T. (1999) The carboxyl terminus of B class ephrins constitutes a PDZ domain binding motif. *J. Biol. Chem.* **274**, 3726-3733
30. Lu, Q., Sun, E.E., Klein, R.S., Flanagan, J.G. (2001) Ephrin-B reverse signaling is mediated by a novel PDZ-RGS protein and selectively inhibits G protein-coupled chemoattraction. *Cell.* **105**, 69-79

31. Lu, Q., Sun, E.E., Flanagan, J.G. (2004) Analysis of PDZ-RGS3 function in ephrin-B reverse signaling. *Methods Enzymol.* **390**, 120-128
32. Marston, D.J., Dickinson, S., Nobes, C.D. (2003) Rac-dependent trans-endocytosis of ephrinBs regulates Eph-ephrin contact repulsion. *Nat Cell Biol.* **5**, 879-888
33. Munthe, E., Rian, E., Holien, T., Rasmussen, A., Levy, F.O., Aasheim, H. (2000) Ephrin-B2 is a candidate ligand for the Eph receptor, EphB6. *FEBS Lett.* **466,** 169-174
34. Nagashima, K., Endo, A., Ogita, H., Kawana, A., Yamagishi, A., Kitabatake, A., Matsuda, M., Mochizuki, N. (2002) Adaptor protein Crk is required for ephrin-B1-induced membrane ruffling and focal complex assembly of human aortic endothelial cells. *Mol Biol Cell.* **13,** 4231-4242
35. Ng, P., Graham, F.L. (2002) Construction of first-generation adenoviral vectors. *Methods Mol Med.* **69**, 389-414
36. Noren, N.K., Arthur, W.T., Burridge. K. (2003) Cadherin engagement inhibits RhoA via p190RhoGAP. *J Biol Chem.* **278,** 13615-13618
37. Noren, N.K., Pasquale, E.B. (2004) Eph receptor-ephrin bidirectional signals that target Ras and Rho proteins. *Cell Signal.* **6**, 655-666
38. Nourry, C., Grant, S.G., Borg, J.P. (2003) PDZ domain proteins: plug and play! *Sci STKE.* **179**, RE7
39. Palmer, A., Zimmer, M., Erdmann, K.S., Eulenburg, V., Porthin, A., Heumann, R., Deutsch, U., Klein, R. (2002) EphrinB phosphorylation and reverse signaling: Regulation by Src kinases and PTP-BL phosphatase. *Molecular Cell.* **9**, 725-737
40. Penzes, P., Beeser, A., Chernoff, J., Schiller, M.R., Eipper, B.A., Mains, R.E., Huganir, R.L. (2003) Rapid induction of dendritic spine morphogenesis by trans-synaptic ephrinB-EphB receptor activation of the Rho-GEF kalirin. *Neuron.* **37**, 263-274
41. Ren, R., Mayer, B.J., Cicchetti, P., Baltimore, D. (1993) Identification of a ten-amino acid proline-rich SH3 binding site. *Science.* **259**, 1157-1161
42. Ribon, V., Herrera, R., Kay, B.K., Saltiel, A.R. (1998) A role for CAP, a novel, multifunctional Src homology 3 domain-containing protein in formation of actin stress fibers and focal adhesions. *J Biol Chem.* **273**, 4073-4080
43. Ridley, A.J. (2001) Rho family proteins: coordinating cell responses. *Trends Cell Biol.* **11** 471-477
44. Riento, K., Ridley, A.J. (2003) Rocks: multifunctional kinases in cell behaviour. *Nat Rev Mol Cell Biol.* **4**, 446-456
45. Saito, H., Minamiya, Y., Saito, S., Ogawa, J. (2002) Endothelial Rho and Rho kinase regulate neutrophil migration via endothelial myosin light chain phosphorylation. *J Leukoc Biol.* **72**, 829-836
46. Salcedo, R., Resau, J.H., Halverson, D., Hudson, E.A., Dambach, M., Powell, D., Wasserman, K., Oppenheim, J.J. (2000) Differential expression and responsiveness of chemokine receptors (CXCR1-3) by human microvascular endothelial cells and umbilical vein endothelial cells. *FASEB J.* **14,** 2055-2064
47. Schmucker, D., Zipursky, S.L. (2001) Signaling downstream of Eph receptors and ephrin ligands. *Cell.* **105**, 701-704

48. Song, J. (2003) Tyrosine phosphorylation of the well packed ephrinB cytoplasmic beta-hairpin for reverse signaling. Structural consequences and binding properties. *J Biol Chem.* **278,** 24714-24720
49. Song, J., Vranken, W., Xu, P., Gingras, R., Noyce, R.S., Yu, Z., Shen, S.H., Ni, F. (2002) Solution structure and backbone dynamics of the functional cytoplasmic subdomain of human ephrin B2, a cell-surface ligand with bidirectional signaling properties. *Biochemistry.* **41,** 10942-10949
50. Stein, E., Lane, A.A., Cerretti, D.P., Schoecklmann, H.O., Schroff, A.D., Van Etten, R.L., Daniel, T.O. (1998) Eph receptors discriminate specific ligand oligomers to determine alternative signaling complexes, attachment, and assembly responses. *Genes and Development.* **12,** 667-668
51. Strawn, L.M. *et al.* (1996) Flk-1 as a target for tumor growth inhibition. *Cancer Res.* **56,** 3540-3545
52. Sturz, A., Bader, B., Thierauch, KH., Glienke, J. (2004) EphB4 signaling is capable fo mediating ephrinB2-induced inhibition of cell migration. *Biochem Biophys Res Commun.* **313,** 80-88
53. Su, Z., Xu, P., Ni, F. (2004) Single phosphorylation of Tyr304 in the cytoplasmic tail of ephrin B2 confers high-affinity and bifunctional binding to both the SH2 domain of Grb4 and the PDZ domain of the PDZ-RGS3 protein. *Eur J Biochem.* **271,** 1725-1736
54. Surawska, H., Ma, P.C., Salgia, R. (2004) The role of ephrins and Eph receptors in cancer. *Cytokine Growth Factor Rev.* **15,** 419-433
55. Tanaka, M., Kamo, T., Ota, S., Sugimura, H. (2003) Association of Dishevelled with Eph tyrosine kinase receptor and ephrin mediates cell repulsion. *EMBO J.* **22,** 847-858
56. Tapon, L., Hall, A. (1997) Rho, Rac and Cdc42 GTPases regulate the organization of the actin cytoskeleton. *Curr Opin Cell Biol.* **9,** 86-92
57. Van Aelst, L., D'Souza-Schorey, C. (1997) Rho GTPases and signaling networks. *Genes Dev.* **11,** 2295-2322
58. Wang, H.U., Chen, Z.F., Anderson, D.J. (1998) Molecular distinction and angiogenic interaction between embryonic arteries and veins revealed by ephrin-B2 and its receptor Eph-B4. *Cell.* **93,** 741-753
59. Woods, D.F., Bryant, P.J. (1991) The discs-large tumor suppressor gene of Drosophila encodes a guanylate kinase homolog localized at septate junctions. *Cell.* **66,** 451-464
60. Zimmer, M., Palmer, A., Kohler, J., Klein, R. (2003) EphB-ephrinB bi-directional endocytosis terminates adhesion allowing contact mediated repulsion. *Nat Cell Biol.* **5,** 869-878

EXTRACURICULAR ACTIVITIES:

- Member of University of Ottawa varsity water polo team: 1999 – Present
  (Captain of the team for the 2001-2002, 2002-2003, 2003-2004 seasons)
- Volunteer for "Let's Talk Science" program, University of Ottawa, 2003 – 2005
- Volunteer water polo coach, Hilcrest High School, Ottawa, 2005
- Member of the University of Ottawa Premed Society: 2000 – 2003
  (VP – Social for the school year 2001-2002
  VP – Finance for the school year 2002-2003)
- Volunteer at Canada Aviation Museum: 2001 - Present
- Member of Carlton Comprehensive High School water polo: 1997 – 1999
- Member of Carlton Comprehensive High School soccer team: 1998 – 1999
- Volunteer water polo coach, Prince Albert Water Polo Club: 1998 – 1999
- Member of Prince Albert Drifters Rowing Club: 1998 – 2000
- School Yearbook Club member, CCHS: 1998 – 1999
- Outdoor Education Club member, CCHS: 1998 – 1999
- Volunteer safety boat driver at Western Canada Summer Games, Prince Albert, 1999

AWARDS AND ACHIEVEMENTS:

- Dean's Honour List, Faculty of Science, University of Ottawa, 2003
- University of Ottawa Science Merit Scholarship, Ottawa, 2003
- University of Ottawa Entrance Scholarship, Ottawa, 1999
- Academic Achievement Award, Ontario University Athletics, (presented in recognition of outstanding academic achievement and athletic performance in Interuniversity sports) Ottawa, 2002
- Friends of Darryl Spencer Award – Valedictorian, Prince Albert, 1999
- I.O.D.E. Athlone Chapter Award (3rd highest average in school), Prince Albert, 1999
- Carlton Science Award, Prince Albert, 1999
- Carlton Mathematics Award, Prince Albert, 1999
- Rhonda Basaraba Memorial Award (presented in recognition of obtaining academic excellence despite having difficulties in life), Prince Albert, 1999
- Gold Team – Chemistry Games: Sports Activities, Quebec, 2002
- Gold Team – Prince Albert Academic High School Challenge, 1999
- Most Valuable Player – Univeristy of Ottawa Water polo Team, Ottawa, 2002, 2005
- Most Inspirational Player award for Water polo, CCHS, Prince Albert, 1998
- Honours with Great Distinction, CCHS, 1999, 1998, 1997
- St. John Ambulance First Aid and CPR, 2001

INTERESTS AND HOBBIES:

- Foreign cultures and languages
- Drawing and modeling airplanes, Reading, movies and music
- Sports: soccer, water polo, volleyball and mountain biking